RC1

Review of
Statistical Analysis of Contrail to Cirrus Evolution during
the Contrail and Cirrus Experiments (CONCERT)

The manuscript presents a new form of statistical analysis, the Principal Component Analysis (PCA), to investigate contrail to cirrus evolution based on two field campaigns. The observed ice clouds are divided in six clusters representative of different development stages of the contrails (primary wake, young contrail, contrail-cirrus and natural cirrus). Optical, chemical and microphysical properties of the clusters are then characterized to describe the ice-cloud properties during contrail to cirrus evolution.
Overall, the paper is very interesting and the topic is timely and suitable for ACP. Especially, the new approach to distiguish contrail and cirrus clouds seems to be promising. The manuscript is well structured and fluently to read. I found a number of minor points that I think needs claryfication before publishing the manuscript, they are listed below.

Nevertheles, my overall rating is major revisions because of two points emphasized here:
– I strongly recommend to include the RHI measurements of flight 19b during CONERT 1. They are published in Gayet et al. (2012), so the data are available – see comment 8).

– Some numbers in Table 2 needs to be checked, the mean and median IWC and, especially, the mean and median of Ntotal for CC are too high for natural cirrus – see comment 20).

We would like to thank the reviewer for his interesting and constructive suggestions. We have tried to follow every suggestion in order to improve the manuscript. Each reviewer's comments are addressed and the manuscript has been modified accordingly.

A significant change in the paper concerns the implementation of an automatic clustering method (k-mean method) to enhance the statistical significance of the contrail phase discrimination. Subsection "*3,2,2 Clustering analyses*" has been added and gives details of the method. After some tests we found that 16 clusters are necessary to classify the patterns revealed by the PCA analysis. To be in accordance with ATC observations, clusters 8 to 16 deduced from the k-mean method (Figure RC2.1.a.) were gathered into two clusters (A and B, Figure RC2.1.b.). Clusters 2 to 5 have also been merged to one single cluster.

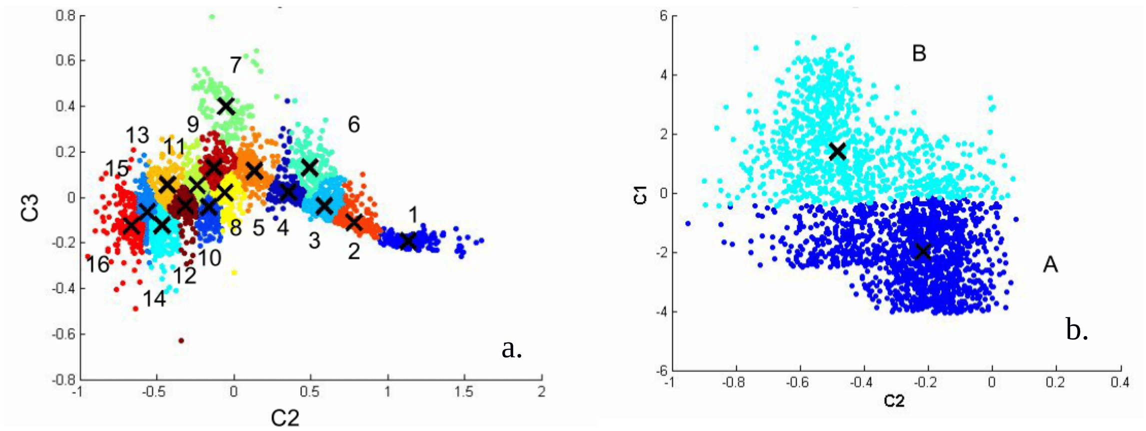

Figure RC1.1.: Clustering analyses according k-mean method. a) First step using 16 clusters and b) second step grouping clusters 8 to 16 to two clusters (A and B).

The following table summarizes the correspondence of the clusters defined by the k-mean methods and the cluster's definitions according to ATC information:

k-mean clusters	Cluster number	definition	name
1	0	Primary Wake	**PW**
6	1	Young Contrail 1	**YC1**
2, 3, 4 and 5	2	Young Contrail 2	**YC2**
A	3	Aged Contrail 1	**AC1**
7	4	Aged Contrail 2	**AC2**
B	5	Cirrus Cloud	**CC**

Table RC1.1: Cluster definitions according the k-mean method.

Comments:

1) Introduction: I like the very detailed introduction, but recommend to introduce more subsections (maybe even with titles), since now there are quite long paragraphs and the structure is not clearly visible.

The structure of the introduction has been changed and two subsections were added, namely:

1.1. Contrail formation and evolution

1.2. Optical and microphysical properties of contrail phases

Moreover, the description of contrail chemical properties has been shortened.

Modifications:

l.55:" *Several studies in the past have been dedicated to the evolution of concentrations of nitrogen oxide (NO) and sulphur dioxide (SO_2) and their oxidized forms (Kärcher and Voigt, 2006 ; Voigt et al., 2006 ; Schäuble et al., 2009 ; Jurkat et al., 2011).*"

2) Page 5, Line 194-195: *Particle size distributions and corresponding microphysical and optical integrated properties (IWC, Deff, N, and extinction) were derived from FSSP-300 measurements (Baumgardner et al., 1992).*

FSSP measurements does not include the larger ice particle and is thus know to be not suitable for calculations of at least IWC and Deff. The 2DC was also flown during the field campaign, so why not combining the two probes for the calculations? The missing size range between the two probes could be interpolated.

Optical and microphysical properties of contrail particles cannot be fully retrieved without the 2DC measurements. In the present study, these properties are retrieved with both instruments, FSSP and 2DC, to consider as much as possible the full-size range of the particle size distribution. The data are linearly interpolated in logarithm space between the two instrument ranges. The text has been clarified according to this remark.

Modifications:

l.191: "*Particle size distributions and corresponding microphysical and optical integrated properties (IWC, Deff, N, and extinction) were derived from both FSSP-300 and 2DC measurements.*"

3) Shattering of large ice crystals is negligible in contrails since the maximum size of the crystals is not large enough to cause this effect. I would mention that somewhere in the manuscript.

Indeed, the shattering of particles with size larger than typically 100µm on the probe inlet can affect the measurements. In addition, this effect can also explain the high number concentrations observed in natural cirrus (Table 3). It is now mentioned in the Manuscript.

Modifications:
l.235: "*These equations do not account for possible shattering of large ice crystals on the probe inlets. This effect is minimized in young contrails but can lead to an overestimation of small ice crystal concentration in contrail cirrus clouds.*"

l.647: "*Besides to interpolation between the FSSP-300 and the 2DC measurements, the assumed shape (spherical or aspherical), and shattering of large ice particles in cirrus and aged contrails can also have a significant effect on the measurement of optical and microphysical properties (Gayet et al., 2012).*"

4) Page 5, lines 220-221: *The bulk parameters were calculated assuming the surface-equivalent diameter relationships of Heymsfield (1972) and Locatelli and Hobbs, (1974).* Which bulk parameters do you mean?

The bulk parameters referred to the IWC, Deff, and extinction. It should be integrated or derived microphysical parameters. It was clarified in the text and, this sentence has been removed and the paragraph modified.

Modifications:
l.221: "*For spherical and non-spherical particles, the extinction coefficients are calculated from the following equation:*

$$Ext = \frac{\pi}{4}\sum_{i} \beta_{ext}^{i} N_i D_i^2 \quad (1)$$

where β^i_{ext} is the extinction efficiency (values depend on spherical or aspherical particle characterization), D_i the mean diameter in channel i, and N_i the number concentration.

Different approaches are used to retrieve ice water content from spherical and non-spherical particles (Garret et al., 2003 ; Gayet et al., 2004 ; Gayet et al., 2012). For spherical particles (gPN > 0.85), IWC is computed from the following equation:

$$IWC_{spherical} = \frac{\pi}{6}\rho_{ice}\sum_{i} N_i D_i^3 \quad (2)$$

with ρ_{ice} the bulk ice density (0.917 g cm^{-3})."

5) Page 6, line 234 - 238 : Calculation of IWC non-spherical : Is the validity of Equ. (6) ever checked by comparison to bulk IWC measurements?

The method used to derive IWC from spherical and non-spherical particles with equivalent diameter calculation, has been validated with different measurement techniques (FSSP-300 and polar Nephelometer) in the work of Gayet et al. (2012). The IWC derived from the particle size distribution is hindered by the uncertainties related to the size dependent enhancement factor for ice crystals in the inlet of total water instruments. There is a strong particle size dependence of the enhancement factor for bulk water instrument inlets in the small particle size range lower than 20 µm representative for young contrails. Further, there is little information on the particle shape effect on the enhancement factor. Finally, the inlet position of bulk phase instruments near the fuselage of the aircraft may introduce additional ambiguities in the IWC measured near the aircraft fuselage. These uncertainties limit the quality of an assessment of the shape effect on the used mass dimension relationship using a comparison to the IWC measurements derived from bulk phase instruments.

6) Page 6, lines 254-256: *In addition, hygrometers using the Lyman-alpha technique (FISH, Zöger et al., 1999; Meyer et al., 2015), and frost point hygrometers (CR-2, Heller et al., 2017) were implemented on the Falcon during CONCERT-1 and 2.*
Please add the names of the hygrometers as indicated in blue.

The two hygrometers names have been added in the text.

Modifications:
l.248: "*(FISH, Zöger et al., 1999; Meyer et al., 2015), and frost point hygrometers (CR-2, Heller et al., 2017) were deployed on the Falcon during CONCERT-1 and 2.*"

7) Figure 1:

a) Caption: Time series at 1 s resolution for flights a) 19b (CONCERT 1) and b) 16b (CONCERT 2).
Please add the names of the campaigns as indicated in blue.

b) Plot of gPN: it would be helpful if a line at 0.85 would be drawn in the figure to better see if the particles are spherical or aspherical.

c) Plot of NO: a log scale might be better here, especially for Flight 19b from CONCERT 1.

All these suggestions have been considered. Figure 1 and its legend have been modified to improve the reading of the figure.

8) Flight 19b from CONCERT 1: Why are the RHI measurements of that flight not included here? They are published in Gayet et al. (2012), so the data are available.

RHI measurements performed during Flight 16b show typically values higher than (or close to) 100% when contrails are detected by the PN (extinction >0.1 km^{-1}). For Flight 19b, RHI values are always higher than 75% but values higher or equal to 100% are scarce. Moreover, contrail/cirrus events identified by the PN or chemical measurements do not seem to be correlated with RHI values. RHI measurements during Flight 19b and CONCERT 1 in general should be taken with caution. An additional bias in the temperature measurements of the Falcon may be responsible for an offset in the RHI measurements inside and outside of contrails during the CONCERT 1. This was not observed during CONCERT 2 where the temperature sensors have been extensively calibrated and RHI peaks near 100% are found in contrails and natural cirrus (Kaufmann et al., 2014). In addition, the descent of the primary wake within the wake vortices leads to an increase in temperature and thus an altitude dependent RHI profile within the contrails as observed by Gayet et al. (2012), Jeßberger et al. (2013) and Kaufmann et al. (2014). Thus, RHI measurements are shown for both campaigns but had to be analysed carefully taking into account the altitude of measurements and calibrations before flights.

Modifications:
RHI measurements for flight 19b (CONCERT 1) are added Figure 1 and Figure 3d.

I strongly recommend to include this data. It can be seen later in the paper that the number of RHI data from only flight 16b from CONCERT 2 is too low to apply the PCA analysis, see Figure 3, bottom right. Further, on page 8, lines 304-305 you write for flight 16 b: *However, no accurate ambient RHI data can retrieved for measurements in natural cirrus due to instrumental calibration problems.* but there are natural cirrus data available for 19b, CONCERT 1, yes?

We apologize for this possible misunderstanding. The PCA is solely based on light scattering measurements performed by the Polar Nephelometer. Other parameters such as RHI or NO concentration are used to validate or evaluate clusters/patterns revealed by the statistical analysis. On the principal component plots (Figure 3), "Natural cirrus" measured during CONCERT 1 are identified based on their scattering properties. Moreover, only one natural cirrus event was observed during flight 16b (none during flight 17) between 17:00 and 17:30. Unfortunately, no RHI measurements were performed during that time.

In addition, on page 6, line 252 you state the importance of RHI to characterize contrail ice crystals and on page 8, 3 rd paragraph, you describe how RHI influences the sphericity of ice crystals. So I think it is of importance not to leave out available RHI measurements!

RHI measurements during CONCERT 1 have been added to the manuscript. Instrumental issues reported in previous works (Kübbeler et al. (2011); Gayet et al. (2012); Jessberger et al. (2013) ; Schumann et al. (2013)) are also mentioned.

Modifications:
l.255: "*RHI measurements during flight 19b as well as instrument shortcomings are discussed in details in Kübbeler et al. (2011), Gayet et al. (2012), Jessberger et al. (2013) and Schumann et al. (2013).*"

9) Page 8, lines 294-297: *In a supersaturated environment of contrails, crystals grow by water vapor deposition and become increasingly aspherical with time. This is why spherical ice crystals prevail in very young contrails with an asymmetry coefficient around 0.85 with RHI above 100%.*

These sentences are a bit confusing. The reason that the ice crystals in young contrails are spherical under supersaturated conditions is that the time was too short to become aspherical, yes ? Maybe better: *In very young contrails, not enough time has passed so that despite RHI is above 100% spherical ice crystals with an asymmetry coefficient around 0.85 prevail.*

Indeed, the previous sentence was not that clear. We have modified the sentence following the reviewer suggestion.

Modifications:
l. 287: "*In a supersaturated environment, crystals grow by water vapour deposition and become increasingly aspherical with time. However, in very young contrails, spherical ice crystals with an asymmetry coefficient around 0.85 prevail.*"

10) Page 8, lines 305-309: *A good example of the evolution of gPN is the CRJ-2 contrail observed between 11:40 and 11:45 during flight 19b. The sequence illustrates the potential of the gPN measurement to characterize the evolution of contrail properties, with decreasing crystal sphericity documented by the decreasing asymmetry parameter from 0.88 to 0.79 (uncertainties around 0.04) after only 5 min and down to 0.77 after 20 min.*
Again, it would be very good to see the corresponding RHI measurements here.

RHI measurements for flight 19b are now added to Figure 1. We can see that despite the presence of a persistent contrail probably due to a supersaturated ambient air, RHI values during this period are too low. Thus, this example shows how the RHI measurements during CONCERT 1 cannot be considered to understand or detect contrail formation.

Modifications:

l. 294: "*However, it is important to note that the RHI measurements during the CRJ-2 chasing events do not show supersaturated conditions, whereas contrail seems persistent. Indeed, RHI measurements should be discussed carefully for this campaign due to calibration issues.*"

11) Page 8/9, last/first paragraph: Correlations between parameters are hard to recognize from Figure 1. Scatterplots for the main correlating parameters (gPN, RHI - from both flights, NO, extPN) would greatly improve the visualization of the discussed relations.

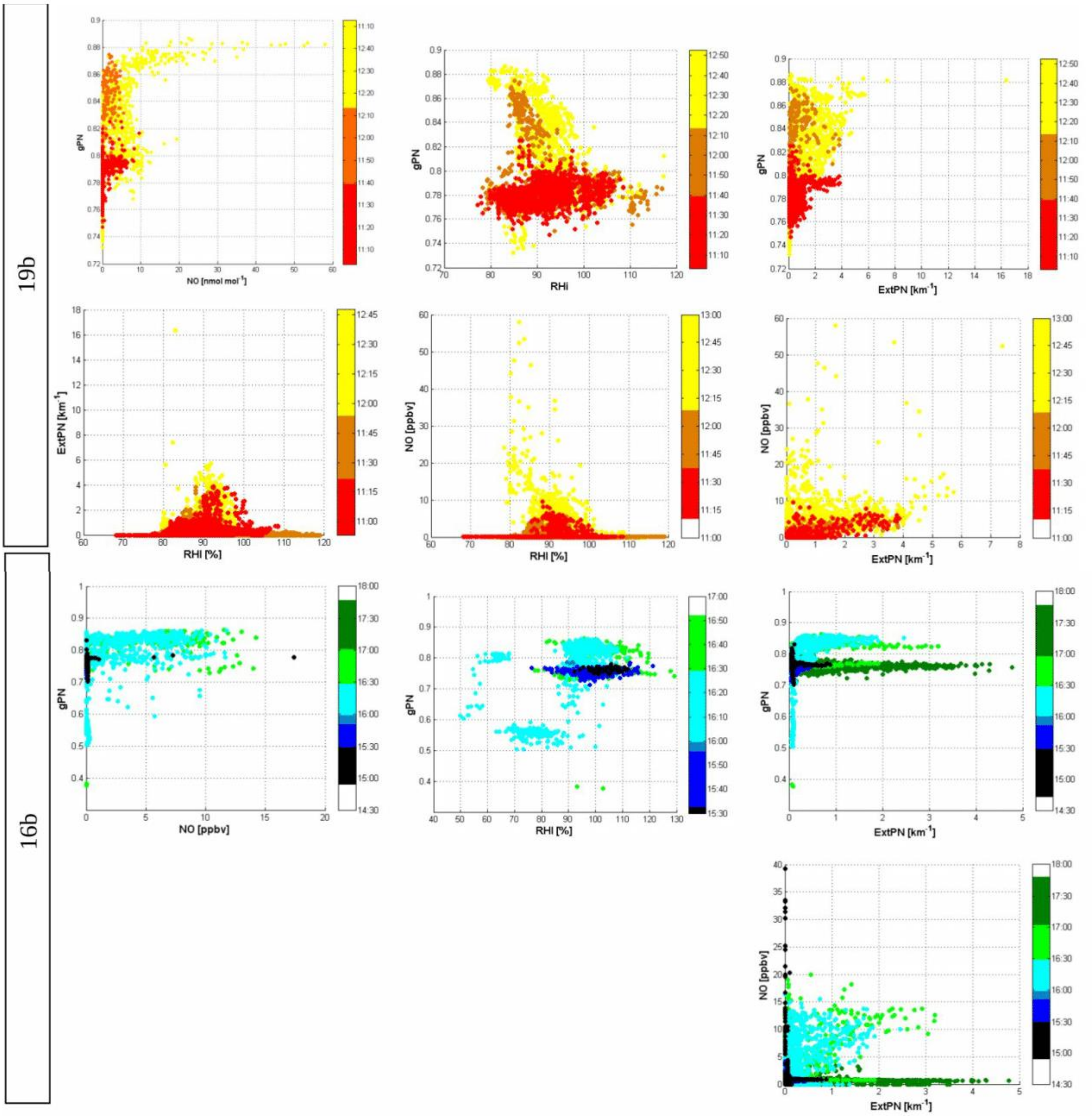

Figure RC1.2.: Correlation between optical and chemical properties during CONCERT 1 and 2 measurement campaign. Colours refers to ATC information for the different chasing and natural cirrus measurements.

The purpose of figure 1 is to illustrate the correlation/correspondence between the main contrail optical and chemical composition trends with ATC information. The only objective of this figure is to help the reader to understand how cloudy and clear sky conditions were determined and to show that parameters like the extinction, the asymmetry parameter and NO concentration can used to identify contrails and cirrus events.
To respond to the reviewer's comment, correlations between extinction, RHI, NO concentration and asymmetry parameter are shown on Figure RC1.2. for 19b and 16b flights. No clear correlations can be seen from these representations since each contrail stages are mixed together. However, NO concentrations and extinction coefficients seem to be linked for particular cases. For clarity, we decided not to show these correlations as it might misguide the reader.

12) Page 12, last paragraph: For a better understanding of this paragraph, I recommend
→ to make a table of the of the cluster numbers and the corresponding definitions (now listed at page 13, lines 453 – 458) and refer to the table at the beginning of the paragraph. In the present form, it is hard to follow the text without knowing the meaning of the numbers.
→ Further, it would be good to note the abbreviations of the numbers (0: PW, 1: YC1, 2: ...) in one panel of Figure 3, e.g. in 3a.

According to reviewer 2 suggestions the clusters have been redefined according Table RC1.1 and abbreviations of the numbers were also added.

Modifications:
The table of cluster definition is added (Table 1). Legends for all subplots has been added in Figure 6 in order to recall each cluster definition.

13) Page 12, line 420-421:
Figure 3a suggests an increase of Cj2 and a decrease of Cj1 with increasing aircraft size.
In Fig. 3a Cj2 vs. Cj3 is plotted, in the text you refer Cj2 vs. Cj1 – please correct.

Because the correlation is not as clear as mentioned in the text, this discussion has been removed from the text.

14) Definition of Clusters 3 (AC: Aged contrail) and 4 (ACC: aged contrail clean):
What is the difference between the two clusters? Does ‚clean means low NO?
Please explain.

"Aged contrail" and "aged contrail clean" can be discriminated based on NO concentrations. "Clean" refers to low NO concentrations compared to measurements corresponding to AC conditions. AC and ACC have been replaced by AC1 and AC2 respectively without taking into account NO concentrations.

15) Figure 4: It would be helpful if you would include the circles from Figure 3 (a) in this plot.

Due to the modification of the clustering method, circles in Figure 3 have been removed. Every cluster's centre is now added on the new Figure 4.

16) Page 14, line 479: attribuate → attribute

The recommendation has been added into the all text.

17) Figure 5: I found it difficult to recognize the message of the panels of Figure 5. Here are some recommendation how this important figure can be improved:
a) in panel (a), a vertical line at gpN=0.85 would be helpful to distinguish between spherical and aspherical.
b) in panel (c), when using a logarithmic scale for the frequency the effects you discuss in the text will become better visible.
c) in panel (d), a logarithmic scale for NO and also the frequency would help to better see the the differences between the clusters.
d) in panel (e), a vertical line at RHI=100% would be good.
Further, in the text it is mentioned that the most frequent value of RHI is 95%. Shouldn‘t that be 100% ? And, the histogram is divided into small RHI intervals (2% ?), but the accuracy of the measurements is not better than 10-20%, I guess. I recommend to divide RHI in intervals corresponding to the accuracy and center them around 100%.
e) How many data points does each cluster contain ? This can be indicated in the legend.
f) The legend could be included in each panel – this would make it easier for the reader to assign the colors to the clusters when zooming the Figure on the screen.
Another idea could be to use more intuitive colors and sort the legend somehow into the stages of development, here a suggestion:
PW YC1 YC2 AC ACC CC

All these recommendations have been considered and included in Figure 6. RHI histogram has been modified to include RHI measurements of CONCERT 1.

18) Page 18, line 592:
Figure 6 shows mean volume particle size distributions (PSD) for all six clusters.
I see mean number PSDs – dN/dlogD19)

We apologize for this mistake, “volume” has been replaced by “number” into the text l.602.

19) Figure 6: The maximum sizes of PW and YC1 are already close to 200 µm, the maximum size of YC2 is close to that of ACC and CC. I would have expected smaller maximum sizes in the PW and YC categories, because ice crystals needs time to grow to larger sizes?
Further, the maximum size of CC is quite small – Voigt et al. (2017) show maximum sizes of natural cirrus PSDs up to 1000 µm or more ? See also comment 19 (b).

Indeed, no particle measurements have recorded up to 1000 µm during the two campaigns. Voigt et al. (2017) show “natural cirrus” and “contrail cirrus” with mean concentrations higher than 0.01 cm^{-3} for particles diameters around 100µm whereas concentrations do not exceed 0.01 cm^{-3} during CONCERT flights at this particle size range. Because instruments are different between the two campaigns, it can be explained by different shattering effects of largest particles, but also by air speed issues as explained in Febvre et al. (2009). In addition, young contrail particles exhibit diameters up to 200 µm. This effect can also be explained by the detection limit of the 2DC instruments which impacts the concentrations for very low signals (50% and 75% for concentrations of 5 and 0.5 cm-3 respectively, Gayet et al., 2002).
This discussion has been added to the text.

Modifications:
PSD measurements from Voigt et al. (2017) and Atlas et al. (2005) have been added to Figure 7.
l. 593: “*PSD measurements in natural cirrus and aged contrails differ significantly depending on the location of the study, ambient air conditions, measurement methods (instrument limitation (Gayet et al., 2002), and air speed (Febvre et al., 2009)). Previous studies show that a 3-hours old contrail cirrus with an effective diameter close to 20 µm (Voigt et al., 2017) and number*

concentration larger than 0.1cm^{-3} (Schumann et al., 2017) can be composed of ice crystals with sizes up to 100 µm (blue dashed line, contrail cirrus figure 7). This differs from the PSD of the natural cirrus presented by Voigt et al. (2017) (dashed black line), which has an order of magnitude lower particle number concentration. In natural cirrus at mid-latitudes, ice crystals with size up to 1600 µm were observed during the ML-CIRRUS campaign (dark dashed line Figure 7, Voigt et al., 2017)."

20) Table 2: (a) I suggest to sort the clusters like recommended under Point 16 f). A further suggestion is to sort Ntotal in two size intervals, namely <~30um and >~30um, since the grouping of the clusters change with size.
(b) The mean and median values of IWC does not fit to each other. For example, for PW / CC the means are 15.46/28.69 mg/m3, but the medians are 6.26/0.96 mg/m3, i.e. the mean of CC is almost twice the mean of PW, but the median of CC is much lower than that of PW ?
Please check all numbers.
(c) Mean/median of Ntotal for CC are 6.06/3.75 cm -3. This is too high for natural cirrus – from Voigt et al. (2017), I would expect something around 0.1 cm -3 or even lower. Is that an arithmetical error , shattering or could it be that contrails are accidentally attributed to CC ? Please clarify!

(a). Table 3 has been sorted according to the development of contrails as proposed by the reviewer in point 16.f).

(b). The new definition of the clusters does not allow to fit mean and median values. This observation may be due to the hypothesis used for PSD definition such as particle sphericity and the interpolation realized between 17 µm and 70 µm.

(c). As mentioned in the previous point, PSD of natural cirrus are significantly different according to measurement location and the different probes used. Here, the new clustering method shows lower number concentrations for the "natural cirrus".

Modifications:
l.623: "*Despite the large uncertainties associated to both instruments and the interpolation between 17 µm and 70 µm diameters, these results again show that each cluster can be connected to a specific contrail phase, and their properties can be compared to previous studies.*"

21) One last comment: could you discuss the possibility to use other/more parameters for the PCA? For example, could Ntotal be included in the PCA ? Or in case no Polar Nephelometer is on board, but PSD, IWC and NO is available, do you think the analysis would be possible?

The present paper demonstrates that the PCA method allows contrail classification from optical properties only. Indeed, additional parameter could improve the performance of the PCA method as PSD measurements, RHI values and NO concentrations. However, the additional parameter should be carefully selected in order to limit the bias introduced by the limitations of the probes and can vary from a measurement campaign to another.
It has been mentioned in the text.

Modifications:
l. 688: "*The additional use of microphysical and chemical measurements can be added to the PCA method in order to improve the selection of contrail phases. Different ranges of extinction or asymmetric coefficients could be also used for PCA analyses in this perspective. However, additional parameters should be carefully selected to limit the bias introduced by the limitations of the probes and the optimal selection may vary from one measurement campaign to another.*"

RC2

Interactive comment on "Statistical Analysis of Contrail to Cirrus Evolution during the Contrail and Cirrus Experiments (CONCERT)" by Aurélien Chauvigné et al.

The authors present aircraft observations of the scattering properties of ice crystals and the trace gas properties sampled inside 17 contrails during two phases of the CONCERT field experiment. While the results presented here are relevant and interesting, the paper has several areas where more explanation is warranted before I can recommend it for publication. For example, some parts of the introduction need to be reorganized.

RC : The most major flaw of the paper which needs to be address is the selection of the clusters. The authors base their cluster classification on a rough examination of the first three principal components in the x-y plane and seem to draw ellipses around where they "roughly identify" where the clusters are. However, with recent advances in machine learning, there are more objective methodologies for classifying data into clusters, with the most applicable methodology for a feature space of three variables to be k-means clustering. The authors should either better justify why their current ellipses were chosen and why the feature space was used for the PCA, or use automated clustering techniques.

Finally, I think a section on how their contrail cirrus observations fit in with past studies is warranted, since the paper lacks much discussion on how their observations fit in with what is already in the literature. I list some other comments below.

We would like to thank the reviewer for his interesting and constructive suggestions. We have tried to follow every suggestion in order to improve the manuscript. Each reviewer's comments are addressed and the manuscript has been modified accordingly.

A significant change in the paper concerns the implementation of an automatic clustering method (k-mean method) to enhance the statistical significance of the contrail phase discrimination. Subsection "*3,2,2 Clustering analyses*" has been added and gives details of the method. After some tests we found that 16 clusters are necessary to classify the patterns revealed by the PCA analysis. To be in accordance with ATC observations, clusters 8 to 16 deduced from the k-mean method (Figure RC2.2.a.) were gathered into two clusters (A and B, Figure RC2.2.b.). Clusters 2 to 5 have also been merged to one single cluster.

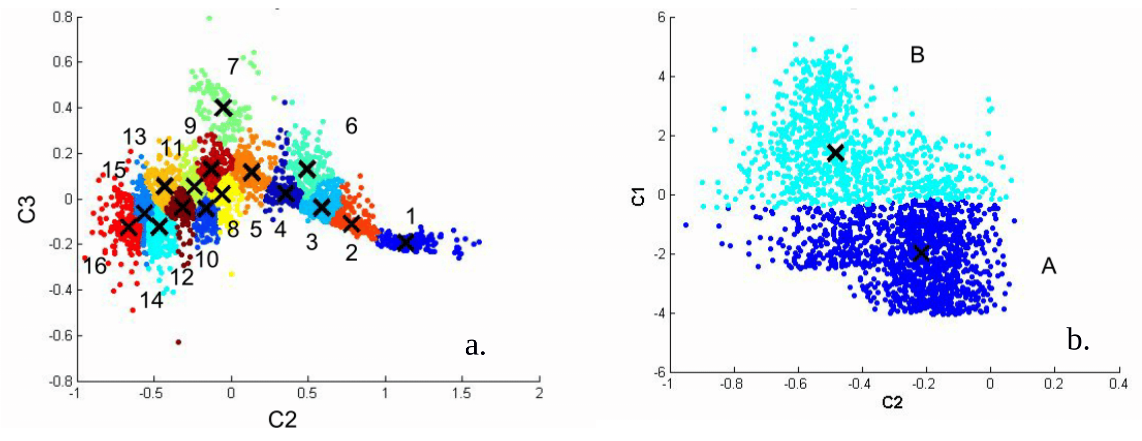

Figure RC2.1.: Clustering analyses according k-mean method. a) First step using 16 clusters and b) second step grouping clusters 8 to 16 to two clusters (A and B).

The following table summarizes the correspondence of the clusters defined by the k-mean methods and the cluster's definitions according to ATC information:

k-mean clusters	Cluster number	definition	name
1	0	Primary Wake	**PW**
6	1	Young Contrail 1	**YC1**
2, 3, 4 and 5	2	Young Contrail 2	**YC2**
A	3	Aged Contrail 1	**AC1**
7	4	Aged Contrail 2	**AC2**
B	5	Cirrus Cloud	**CC**

Table RC2.1: Cluster definition according the k-mean method.

Comments:

Major comments:
Lines 51-91. This paragraph is too long and needs to be reorganized. For example, there is too much detail on how NO from aircraft exhaust is converted into acids that does not really add to the major point that NO interacts with OH to make nitr(ic)ous + sulfuric acid. I also feel that this can really be 3 paragraphs: one about NO interacting with OH to produce acids, one about the contrail production process and one about the contrail aging process.

The structure of the introduction has been changed and two subsections were added, namely:

1.1. Contrail formation and evolution
1.2. Optical and microphysical properties of contrail phases

Moreover, the description of contrail chemical properties has been shortened.

Modifications:
l.55: "*Several studies in the past have been dedicated to the evolution of concentrations of nitrogen oxide (NO) and sulphur dioxide (SO_2) and their oxidized forms (Kärcher and Voigt, 2006 ; Voigt et al., 2006 ; Schäuble et al., 2009 ; Jurkat et al., 2011).*"

Line 109-146: I feel that a lot of the individual data points cited here are better suited for an extra section in the paper comparing your contrail observations against past studies. Right now, no link is made to how your categories compare against these past observations and I think such a comparison is needed in order to justify that the range of values that you observe in your clusters correspond to contrails properties that are observed in nature. Therefore, I recommend shortening this paragraph to
just briefly explain how the microphysical properties of contrails evolve with time with leaving specific numbers to a later comparison.

The paragraph has been shortened and we compared our contrail observations against past studies in section 4.2. In particular, average microphysical properties of the clusters were compared with the main findings of Voigt et al. (2017), Schumann et al. (2017) and Atlas et al. (2005). We also discussed the shortcomings related to the interpolation of the PSD and its impact on the derived microphysical quantities.

Modifications:

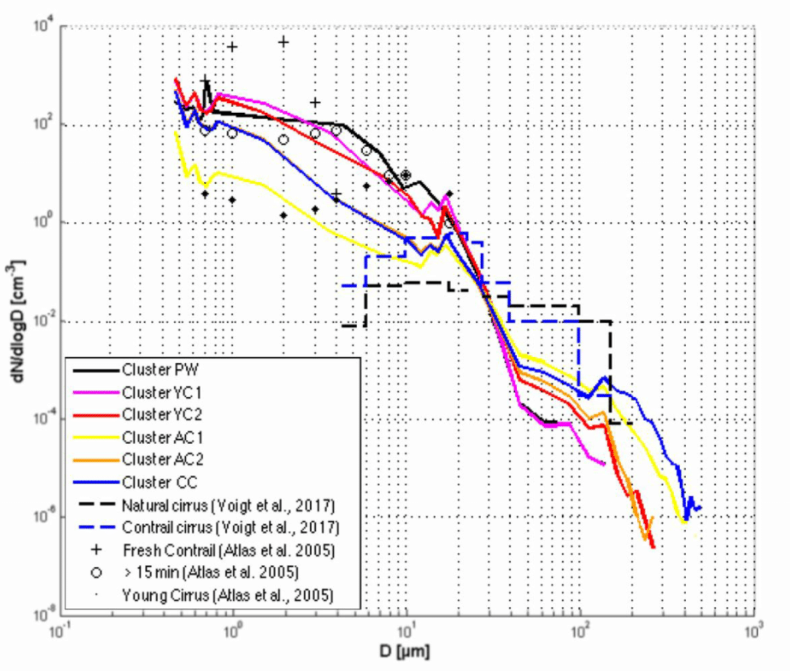

Figure 7: Number particle size distributions for each cluster including all data points of all flights. FSSP-300 measurements from 0.5 to 17 µm and 2DC measurements from 70 µm to 800 µm. The data are linearly interpolated in logarithm space between 17 µm and 70µm.

Voigt et al. (2017) and Atlas et al. (2005) PSD measurements have been added to Figure 7 to get a better picture of previous results. It should strengthen the statements on contrail properties discussed in this section.

l.591:"*Because of this gap, the derived microphysical properties should be considered with caution, but may be used to check the cluster definitions.*"

l. 595: "*Previous studies show that a 3-hours old contrail cirrus with an effective diameter close to 20 µm (Voigt et al., 2017) and number concentration larger than 0.1cm^{-3} (Schumann et al., 2017) can be composed of ice crystals with sizes up to 100 µm (blue dashed line, contrail cirrus figure 7). This differs from the PSD of the natural cirrus presented by Voigt et al. (2017) (dashed black line), which has an order of magnitude lower particle number concentration. In natural cirrus at mid-latitudes, ice crystals with size up to 1600 µm were observed during the ML-CIRRUS campaign (dark dashed line Figure 7, Voigt et al., 2017).*"

l.630: "*These properties are in agreement with previous measurement reported by Gayet et al. (2012) with particle number concentrations close to 200 cm^{-3} for contrails less than 60 s after their formation. Their work also reports extinction coefficient around 7 km^{-1} presenting the highest values of the contrail life time.*"

l.638: "*The ice number concentrations are in agreement with previous results with values between 200 and 100 cm^{-3} for contrail ages between 60 s and 3 min, and around 5 cm^{-3} for contrail ages around 10 min (Goodman et al., 1998 ; Lawson et al., 1998 ; Schröder et al., 2000 ; Schäuble et al., 2009 ; Gayet et al., 2012 ; Voigt et al., 2017).*"

l.645: "*However, the ice number concentration and the extinction coefficient are higher than in previous studies, with values around 0.1 cm^{-3} and 0.023 km^{-1} respectively.*"

Line 223-225: You aren't using the 2DC for calculating IWC though! I don't see why this sentence is needed. However, I think text here justifying why you are not using observations below 70 microns due to the 2DC's limited response time and depth of field need to be here.

Optical and microphysical properties of contrail particles cannot be fully retrieved without the 2DC measurements. In the present study, these properties are retrieved with both instruments FSSP and 2DC, to consider as much as possible the full size range of the particle size distribution. A linear interpolation has been applied between the two instrument ranges. The text has been clarified according to this remark.

Modification:
l.191: "*Particle size distributions and corresponding microphysical and optical integrated properties (IWC, Deff, N, and extinction) were derived from both FSSP-300 and 2DC measurements.*"

Section 3.2: I think more justification needs to be given for the choice of your feature space for the PCA, since right now it is presented without really linking the feature space to looking for quantities that we expect to vary in differing stages of contrail cirrus. For example, why did you conduct a PCA on the entire scattering phase function instead of just apply clustering to the asymmetry parameter?

Also, why were the clusters manually chosen instead of using automated techniques like k-means clustering?

We thank the referee for this very interesting point and for the new perspective brought to the interpretation of our results. The k-mean clustering method was applied to our dataset. We found that this clustering method lead to an accurate (and more robust) classification of every contrail phase and natural cirrus which agrees with ATC information.
The asymmetry parameter information is not sufficient to define the different clusters (Jourdan et al., 2010). Indeed, gPN information cannot be used to separate the group YC1/YC1 and AC1/AC2/CC, which represent the most interesting part of the study. Additionally, Jourdan et al. 2010 and 2003 showed that the asymmetry parameter alone cannot represent or mimic the variability of the phase function. Indeed, the information content of a phase function measurement can be used to discriminate ice clouds characterized by different ice crystal shape, size or degree of surface roughness which is not the case with the g factor alone. Our study here clearly shows that the first 2 principal components (which are correlated to the extinction coefficient and the g factor respectively) cannot reproduce the whole variability of the optical (and microphysical) properties. The third principal component adds additional valuable information on contrail type which is not directly related to the asymmetry parameter.

Modifications:
The k-mean method has been applied to the dataset and an additional subsection has been added ("*3,2,2 Clustering analyses*). The new clusters are thus defined as mentioned above.

Lines 505-512: How do you know that you flew in an aged contrail with no verification from ATC? I think the important conclusion here is more that, microphysically, aged contrails and cirrus are very similar and are difficult to distinguish with this data alone.

For flight 17 of CONCERT 2, ATC reports chasing but without any possibility to check which aircraft is actually followed. This information indicates that measurements may correspond to very aged contrails or natural cirrus. From in-situ measurements, aged contrails and natural cirrus are very similar. In our case, the PCA method along with K-mean clustering method classifies the 17 C-2 measurement in both aged contrail and natural cirrus (AC1 and CC) with both a significant number of point. This can be explained by a limitation of the method to separate aged contrail and natural cirrus due to quite similar optical properties, but also by a mixture of both natural cirrus and aged contrails. Indeed, differences exist in the [60°-80°] range as well as in the forward and backward scattering regions. These differences can be significant as they are detected by the PCA and the clustering method.

Modifications:
l.505: "*Still ATC data indicate measurements in exhaust plumes and the Falcon flew apparently in visible contrails (ExtPN > 0.1 km^{-1}) which were probably too old for ATC recognition.*"

Line 518-522: I think this analysis can be better supported by showing the distributions of contrail ages from ATC.

Only an estimation of contrail age range is available. We couldn't derive a precise age for each individual contrail sampled during each flights. Table 2 shows the available age ranges for the identified contrails.

Line 593-595: I would not interpolate data in this range since the interpretation of extrapolated data could be quite dangerous. I would simply state that concentrations in this size range are too uncertain to report due to the 2DC's poorly characterized depth of field and response time.

We agree with this comment as the interpolation between the two instruments can induce large uncertainties when calculating the microphysical properties. However, we choose to keep this approximation in order to retrieve microphysical properties comparable to previous studies.

Modifications:
l.623: "*Despite the large uncertainties associated to both instruments and the interpolation between 17 µm and 70 µm diameters, these results again show that each cluster can be connected to a specific contrail phase, and their properties can be compared to previous studies.*"

Lines 607-610: Your YC1 contrails seem to have roughly similar 2DC number concentrations to the aged contrails. Why is that?

The new clustering method refined the cluster definition. Consequently, it leads to a better partitioning of contrail microphysical properties. Indeed, as shown by the new Figure 7, the mean PSD from cluster YC1 displays significantly less particle in the 2DC measurement size range than the one corresponding to AC1 and AC2 clusters.
As already discussed into the text, differences between each mean PSD should be taken carefully due to uncertainties of both probes.

Modifications:
These discussion has been added into the text l.616:"*Within the 2DC range, the PSDs are also in agreement with the cluster definitions. A higher concentration of large ice crystals with diameters around 100 µm and larger are expected for natural cirrus (cluster CC) and for significantly well-developed contrails. This is particularly well illustrated by the mean PSD from cluster YC1 that*

displays significantly less particles in the 2DC measurements size range than the one corresponding to AC1 and AC2.”

Lines 640-667: I would convert this into a bulleted list of conclusions to make this paragraph easier to read.

A summary of contrail property is more clearly presented in two separate paragraphs on the conclusion.

Figures/Tables:

Figures 5c,d: A logarithmic x-axis would make the lines easier to distinguish.
Figure 6: I would advise removing the lines where you don’t have the PSD from the two probes in the ~20 to 70 micron range. Can you also add size distributions from past studies and include them in the comparison?

Table 2: I think some data from contrails sampled in past studies should be shown and compared against here and in the paragraph discussing Table 2.

Figure 6 c,d : The suggested modifications have been taken into account.

Figure 7: Previous PSDs (Voigt et al., 2017 and Atlas et al., 2005) have been added to the Figure as reported in previous comments of the reviewer. However, we believe that interpolation illustrations at this stage of the paper is essential in order to understand microphysical properties retrieved from this approximation.

Table 3: Results from past studies are now discussed in the text.

Statistical Analysis of Contrail to Cirrus Evolution during the Contrail and Cirrus Experiments (CONCERT)

Aurélien Chauvigné[1], Olivier Jourdan[1], Alfons Schwarzenboeck[1], Christophe Gourbeyre[1], Jean François Gayet[1], Christiane Voigt[2,3], Hans Schlager[2], Stefan Kaufmann[2], Stephan Borrmann[3,4], Sergej Molleker[3,4], Andreas Minikin[2,5], Tina Jurkat[2], Ulrich Schumann[2]

[1]Laboratoire de Météorologie Physique, UMR 6016 CNRS/Université Clermont Auvergne, Clermont-Ferrand, France.
[2]Institut für Physik der Atmosphäre, Deutsches Zentrum für Luft- und Raumfahrt (DLR), Oberpfaffenhofen, Germany.
[3]Institut für Physik der Atmosphäre, Universität Mainz, Mainz, Germany.
[4]Max-Planck-Institute for Chemistry, Department for Particle Chemistry, Mainz, Germany.
[5]Now at: Flugexperimente, Deutsches Zentrum für Luft- und Raumfahrt (DLR), Oberpfaffenhofen, Germany.

~~-~~**Abstract:**

Air traffic affects the cloudiness, and thus the climate, by emitting exhaust gases and particles. The study of the evolution of contrail properties is very challenging due to the complex interplay of vortex dynamics and atmospheric environment (e.g. temperature, supersaturation). Despite substantial progress in recent years, the optical, microphysical, and macrophysical properties of contrails and ambient cirrus during contrail formation and subsequent ageing are still subject to large uncertainties due to instrumental and observational limitations and the large number of variables influencing the contrail life cycle. In this study, various contrail cases corresponding to different aircraft types and atmospheric conditions are investigated using a statistical method based on the in situ optical measurements performed during the CONCERT campaigns 2008 and 2011. These two aircraft campaigns encompass more than 17 aircraft contrail cases. A Principal Component Analysis (PCA) of the angular scattering coefficients measured by the Polar Nephelometer ~~has been~~is implemented~~ in order~~. The goal is to classify the sampled ice cloud measurements in 6 clusters representative of different contrail development stages ~~of the contrails~~ (primary wake, young contrail, contrail-cirrus and natural cirrus). ~~Based on the information derived from air traffic control, extinction coefficients~~ Extinction and, asymmetry coefficients, nitrogen oxide concentrations, relative humidity with respect to ice (RHI) and particle size distributions are ~~analyzed~~analysed for each cluster to ~~provide a characterization of~~characterize the evolution of ice-cloud properties during the contrail to cirrus evolution. The PCA demonstrates that ~~-~~contrail optical properties are well suited to identify and discriminate the different contrail growth stages and to ~~provide an independent method for the characterization of~~characterize the evolution of contrail properties.

1 Introduction

Aircraft exhaust plumes have a significant impact on climate and tropospheric chemistry (Lee et al., 2010; IPCC, 1999). The Intergovernmental Panel for Climate Change IPCC special report on aviation (1999) estimates that NO_x emissions from subsonic aircraft increase ozone concentrations

~~by up to 6%~~ at cruise level. Short and long lived pollution species have different impact on atmospheric chemical composition depending on the flight level (Frömming et al, 2012). Emissions of water ~~vapor~~vapour, black carbon (BC) / soot particles, ~~sulfate~~sulphate (SO_4) aerosols and nitrogen oxides (NO_x) contribute to the modification of the chemical composition of the upper troposphere on shorter timescales (Lee et al., 2010, Gettelman and Chen, 2013; Liou et al., 2013). The long~~-~~-term climate impact is mainly driven by CO_2 emissions. Modelling studies have shown that the direct radiative forcing from aviation is expected to represent 3-4% (50-60 mW m^{-2}) of the anthropogenic forcing (Lee et al., 2010; De Leon et al., 2012) and could reach 87 mW m^{-2} in 2025 ~~(Chen and Gettelman, 2016).~~(Chen and Gettelman, 2016). Aircraft induced cloudiness has also an important impact on climate, although the quantitative assessment of the radiative forcing remains a major source of uncertainties (Lee et al., 2010).

1.1. Contrail formation and evolution

Contrail formation is mainly controlled by the thermodynamic properties of the ambient air and by the aircraft emissions. The conditions for contrail formation can be determined by the Schmidt-Appleman Criterion (SAC) (Schumann, 1996). Contrail chemical composition can have a significant impact on the contrail formation (Kärcher et al., 2009). Indeed, the ~~emission index (e.g. soot emission index in kg-fuel^{-1}) is directly linked to the~~ contrail microphysical properties, as the total number densities and ice crystal diameters~~.~~, are directly linked to the emission index (e.g. soot emission index in kg-fuel^{-1}). Several studies in the past have been dedicated to the evolution of concentrations of nitrogen oxide (NO) and ~~sulfur dioxide (SO_2). Rapidly oxidized by OH (post-combustor reaction; Jurkat et al., 2011), NO and SO_2 are transformed into a series of species including nitrous acid (HONO), nitric acid (HNO_3), and sulfuric acid (H_2SO_4). Part of the nitric acid, e.g., formed in the young plume is taken up by contrail ice particles (Kärcher and Voigt, 2006; Voigt et al., 2006; Schäuble et al., 2009). HONO can be a temporary reservoir of OH by photolysis reactions, and H_2SO_4 a precursor for radiatively active sulfate particles also contributing to soot particle coating (Jurkat et al., 2011). OH-induced reactions, formation and reaction schemes of greenhouse gases (H_2O, O_3, CH_4), as well as emission of black carbon and sulfate aerosols have significant impact on climate (Frömming et al., 2012; Gettelmann and Chen, 2013).~~ sulphur dioxide (SO_2) and their oxidized forms (Kärcher and Voigt, 2006 ; Voigt et al., 2006 ; Schäuble et al., 2009 ; Jurkat et al., 2011).

Two different processes of contrail formation have been studied: combustion condensation trails and aerodynamic condensation trails. Different studies (Gierens and Dilger, 2013; ~~Jansen and Heymsfield, 2015)~~Jansen and Heymsfield, 2015) have illustrated characteristics of aerodynamically controlled contrail formation associated to warmer temperatures (observations at temperatures above -38°C). ~~For~~ Contrails primarily initiated by the combustion processes~~,~~ result from the mixing of hot and humid exhaust gases with cooler and dryer ambient air. This increases the local relative humidity in the exhaust plume leading to the formation of contrails when the saturation with respect to liquid water is reached. ~~Thus~~In this case, soot and ~~sulfate~~sulphate aerosols emitted by the aircraft (Moore et al., 2017) may act as condensation nuclei to form liquid droplets. Homogeneous ice nucleation of the liquid droplets can occur when the exhaust cools down through mixing with the ambient temperature, while preserving ice saturation. Small ice crystals are then formed in the jet phase within some tenths of a second (Kaercher and Yu, 2009).

The ~~further~~ life-cycle of contrails depends on the interaction with the wake vortices behind aircraft and the ambient atmosphere (Irvine et al., 2012; Graf et al., 2012; Duda et al., 2013; Carleton et al., 2013; Schumann and Heymsfield, 2017). The ice crystals in the young contrails are captured within two counter-rotating wake vortices in the downwash behind the aircraft induced by the aircraft lift, which induce adiabatic compression, heating, and partial sublimation of the ice crystals within the primary wake (Lewellen and Lewellen, 2001; Sussmann and Gierens, 2001, Unterstrasser et al., 2008, Unterstrasser et al., 2016; Kärcher and Voigt, 2017). This primary wake may soon disappear if ambient air is subsaturated with respect to ice. In the case of supersaturation, the secondary wake becomes visible, thereby detraining ice particles from the primary wake at a higher level (Sussmann and Gierens, 1999, Kaufmann et al., 2014). The initially almostQuasi spherical ice crystals become increasingly aspherical and grow by uptake of water vaporvapour as long as saturation with respect to ice is prevailing. For ambient humidity above ice saturationInice saturated conditions, contrails can persist after the vortex breakdown, spread and evolve into contrail cirrus (Schumann and Heymsfield, 2017). The associated cloud cover (larger than for linear contrails alone) increases thes radiative forcing of contrail cirrus then shows increasing impact on the radiative forcing (Burkhardt and Kärcher, 2011; Schumann et al., 2015).

1.2. Optical and microphysical properties of contrail phases

The assessment of the contrail radiative forcing requires, in particular, an accurate estimation of the cloud cover, the visible optical depth, the single scattering characteristics, the ice crystal effective size and habit (Yang et al., 2010; Spangenberg et al., 2013). Satellite observations provide a comprehensive dataset to study statistically the contrail to cirrus evolution. The combined contrail tracking algorithms on the Spinning Enhanced Visible and Infrared Imager (SEVIRI) on board the Meteosat Second Generation (MSG) satellites with properties inferred by the Moderate Imaging Spectroradiometer (MODIS) on board the Terra satellite was used by Vazquez-Navarro et al., (2015)Vazquez-Navarro et al., (2015) to characterize the properties of 2300 contrails. Properties included lifetime (mean values of 1h), the width (8 km), the length (130 km), the optical thickness (0.34), the altitude (11.7 km) and the radiative forcing (-26 W m^{-2} for shortwave forcing over land) of these contrails.

However, detailed in situ optical and microphysical measurements are still needed to evaluate satellite products and to develop more appropriate retrieval algorithm. In particular, distinguishingDiscriminating contrails from natural cirrus from satellite observations remains extremely challenging from satellite observations. Although the optical and microphysical properties of young contrails (linear contrails) differ from natural cirrus properties, the contrail properties are highly time dependent and persistent contrail cirrus can be embedded in thin cirrus clouds. Recent *in situ* measurements (Voigt et al., 2017) show that the microphysical properties of contrail cirrus can still be distinguished from natural cirrus at contrail cirrus ages up to several hours.

Most of the studies (Jessberger et al., 2013; Lewellen et al., 2012; Schumann et al., 2013) separate the contrail analysis between the two wakes. Indeed, the ; Schumann et al., 2013) separate the contrail analysis between the two wakes. Primary and secondary wake properties depend strongly on atmospheric conditions and aircraft type (emission index, vortex, flight level, ambient humidity, temperature,…).., …). In the primary wake, contrail ice crystals are quasi-spherical with values of the effective diameter (Deff) typically lower than 4 µm (Schumann et al., 2011; Gayet et al., 2012; Järvinen et al., 2016; Schumann et al., 2017b). Also The total number concentration of ice particles is typically larger than 1000 cm^{-3} a few seconds after contrail formation (Baumgardner and Gandrud, 1998; Petzold et al., 1997) and subsequently). Then, it decreases by dilution to concentrations below 200 cm^{-3} within less than a minute after contrail generation (Poellot et al., 1999; Schröder et al., 2000; Gayet et al., 2012). Gayet et al. (2012) reported mean values of ice water content of 3 mg m^{-3} and maximum extinction coefficients close to 7 km^{-1}. The recent overview on contrail studies presented in Schumann et al. (2017b) reports several microphysical In agreement with these results, the recent overview on contrail studies presented in Schumann et al. (2017b) reports several microphysical properties at different stages, for different atmospheric conditions as well as comparisons with the

Contrail Cirrus Prediction (CoCIP) model simulations. Their study also highlights a large variability (which increases with contrail age) of contrail properties.~~ Comparing primary and secondary wakes,~~

Several studies reported findings on the secondary wake and its evolution into contrail cirrus. Detrained from the primary wake and submitted to saturated ambient air with respect to ice, ice crystals grow rapidly, while crystal concentration decreases. Within the first minutes after formation, measurements exhibit aspherical ice crystals characterized by effective sizes up to 6 µm, IWC ranging between 2.5 and 10 mg m^{-3}, extinction between 2 and 3 km^{-1}, with crystal concentrations typically lower than 100 cm^{-3} (Goodman et al., 1998; Voigt et al., 2010; Kübbeler et al., 2011; Gayet et al., 2012; Jeßberger et al., 2013; Schumann et al., 2013; Poellot et al., 1999; Febvre et al., 2009; Kaufmann et al., 2014). Aged contrails can persist and evolve into contrail cirrus if the ambient air is saturated with respect to ice, however those studies are limited by the lack of unambiguous identification (Schumann et al., 2017a). ~~Also~~

After a few minutes, ~~difficulties appear for the pilot to track the contrail~~tracking contrails by visual navigation~~, which~~ is ~~due to~~challenging as contrail and contrail cirrus ~~spreading~~spread in the free troposphere. Observations of the ice crystal shape and growth over several tens of minutes and up to an hour illustrate that crystal effective size can easily reach 20 µm and beyond with number concentrations ranging from 1 to 5 cm^{-3} (Lawson et al., 1998; Schäuble et al., 2009), extinction less than 0.5 km^{-1} (Febvre et al., 2009), and IWC up to 10 mg m^{-3} (Schröder et al., 2000; De Leon et al., 2012). At this stage, within a sustained ice-supersaturated environment, contrail microphysical properties may still differ from those of natural cirrus (Voigt et al., 2017) with concentrations of ice crystals larger than 100 µm in the order of 0.1 cm^{-3}. These crystals typically show bullet rosette type habits (Heymsfield et al., 1998; Heymsfield et al., 2010). Optical depth values can reach ~~a value~~values of 2.3 (Atlas and Wang, 2010), corresponding to an extinction of 0.023 km^{-1}. Nevertheless, the transition from contrails to cirrus highly depends on the ambient saturation conditions~~ and modelling studies with typical atmospheric conditions suggest time evolution of optical and microphysical properties from contrail to contrail cirrus clouds (Burkhardt and Kärcher, 2011;~~. Modelling studies with typical atmospheric conditions show a temporal evolution of the optical and microphysical properties when contrails evolve to contrail cirrus clouds (Burkhardt and Kärcher, 2011; Unterstrasser et al., 2016 ; Schumann et al., 2015).

In this study, we report on a ~~method presenting a~~ powerful alternative ~~for classifying~~to classify cloud events into young contrail, contrail-cirrus and natural cirrus. The method is applied to aircraft data of the CONCERT (Contrail and Cirrus Experiment) campaigns (Voigt et al., 2010, 2011, 2014). The methodology consists ~~of~~in implementing a Principal Component Analysis (PCA) of the angular light scattering data ~~from a~~ measured by the Polar Nephelometer. The PCA ~~results of the~~ patterns are classified to yield different ~~type of contrails (different clusters) are then utilized with~~cluster representing specific contrail types. Corresponding optical, microphysical, and chemical properties ~~in order to validate hypothesis on~~are derived for each contrail phase ~~definitions ((~~from young contrails to cirrus contrails). This paper starts with an ~~illustration~~overview of the properties of contrails and cirrus clouds observed during two specific CONCERT flights (19 November 2008 and 16 September 2011) encompassing a series of different contrail evolution ~~phases~~stages. These two flights containing a variety of contrail-cirrus information can be regarded as an analytical framework producing results which then can be compared to contrail-cirrus properties of other flights.

2 CONCERT projects and data processing

2.1 CONCERT campaigns

CONCERT-1 and CONCERT-2 campaigns took place in October/November 2008 and August/September 2011, respectively. These two campaigns with the DLR Falcon 20 E research aircraft were based in Oberpfaffenhofen, Germany, and sampled contrails and cirrus at mid-latitudes ~~in the Northern Hemisphere.~~over Europe. The overall objective ~~has been~~was to reduce uncertainties on the microphysical, chemical, and radiative properties of contrails behind aircraft of different types and to improve the evaluation of contrail's impact on climate. ~~Besides the primary objectives focusing on contrails,~~A few CONCERT flights were also dedicated to study emissions of Etna and Stromboli volcanos (Voigt et al., 2014; Shcherbakov et al., 2016). ~~Also~~ A few stratospheric intrusions were also observed during the flight missions. In total, 23 flights were recorded during the two measurement campaigns, wherein 12 flights were entirely focused on aircraft contrail chasing. Overall, more than 17 different aircraft exhausts plumes have been probed. ~~Particularly, the~~ CONCERT-2 campaign mainly focused on ~~observing~~the observation of persistent contrails, and hence on the evolution of contrails ~~into~~to contrail cirrus.

During both CONCERT campaigns, the DLR research aircraft Falcon was equipped with a set of instruments to measure the optical and microphysical properties of cloud particles and also the trace gas composition in the UTLS (Upper Troposphere / Lower Stratosphere) region. Voigt et al. (2010) provide a detailed description of the aircraft instrumentation. We briefly introduce the instruments used in this study.

2.2 Aircraft instrumentation

The microphysical and optical particle properties of contrails and cirrus presented in this study were mainly derived from the PMS Forward Scattering Spectrometer Probe 300 (FSSP-300), the Polar Nephelometer (PN), and the PMS 2D-C hydrometeor imaging probe. The combination of these independent techniques characterizes cloud particles within a range of diameters varying from 0.5 µm to 2 mm.

The PN (Gayet et al., 1997) measures the angular scattering coefficients (non-normalized scattering phase function) of an ensemble of water droplets or ice crystals or a mixture of those particles ranging from a few micrometers to approximately 1 mm in diameter. These particles intersect a collimated laser beam, at a wavelength of 804 nm, near the focal point of a parabolic mirror. The light scattered at angles from 3.49° to 172.5° is reflected onto a circular array of 56 near-uniformly positioned photodiodes. In this study, reliable measurements were performed at 30 scattering angles ranging from ±15° to ±162°. ~~The measurements allow to distinguish~~ Particle phase (water droplets and/or ice crystals) ~~and to derive~~can be assessed as well as single scattering properties such as the extinction coefficient and the asymmetry coefficient with uncertainties of 25% and 4%, respectively (Gayet et al., 2002; Jourdan et al., 2010).

Particle size distributions and corresponding microphysical and optical integrated properties (IWC, Deff, N, and extinction) were derived from both FSSP-300 and 2DC measurements. The FSSP-300 (Baumgardner et al., 1992~~). This instrument~~) measures the intensity of forward scattered light from cloud particles passing through the laser beam, with cloud particles in the diameter range 0.35-20 µm. In the forward angular region (from 4° to 12°), scattering is mainly described by the particle diffraction pattern and therefore depends on the refractive index, the shape, and the size of the particles. The method of data processing and size calibration used during the CONCERT campaigns have been presented in Gayet et al. (2012~~) (Appendix A~~). We briefly recall that the asymmetry parameter derived from the PN was used to discriminate nearly spherical particles ($g \geq 0.85$) from non-spherical ones ($g < 0.85$) at 804 nm. For spherical ice particles, Mie calculations were used to derive the size bin limits and the corresponding extinction efficiency. Results were adjusted to the calibrated probe response. Additionally,~~ in order~~ to minimize Mie ambiguities related to the FSSP-300 size response, 31 channels were rebinned to 13 channels with a diameter ranging from 0.5 µm to 18 µm (upper channels 30 and 31 were excluded from the data analysis). For non-spherical particles, the size of the contrail particles is expressed in terms of an equivalent surface or area diameter, i.e. the diameter of a sphere that has the same area than the projected area of the measured non- spherical particle image (Mishchencko et al., 1997; Schumann et al., 2011). The particles were assumed to be rotationally symmetric ice ellipsoids with an aspect ratio of 0.5. Accordingly, and contrary to the method used for spherical particles, 15 size bins ranging from 0.5 µm to 18 µm were defined based on T-Matrix calculations following Borrmann et al., (2000).

The bi-dimensional optical array spectrometer probe (2DC) provides information on the crystal size and shape within a nominal size range from 25 µm to 800 µm by recording cloud particles shadow images with a 25 µm resolution. The method of data processing used in this study is described in detail in Gayet et al. (2002) and Febvre et al. (2009). Reconstruction of truncated particles has been considered for the PSD calculations and the sampling surfaces have been derived according to Heymsfield and Parrish (1978). ~~In order~~ To improve the statistical significance of low particle concentrations, a 5-s running mean was applied. ~~The bulk parameters were calculated assuming the surface-equivalent diameter relationships of Heymsfield (1972) and Locatelli and Hobbs, (1974).~~ As the sensitivity of the probe to small particles decreases with airspeed (Lawson et al., 2006), particles smaller than 100 µm may not be detectable at the Falcon airspeed of typically 180 m s^{-1}. This may result in larger uncertainties of up to 100% in the derived microphysical parameters such as the IWC (Gayet et al., 2002 and 2004).

~~Depending on the~~For spherical ~~or~~and non-spherical ~~shape of ice crystals, ice water content IWC,~~ particles, the extinction ~~coefficient Ext, and effective diameter D_{eff} were calculated independently according to Garret et al. (2003) and Gayet et al. (2012). For spherical ice crystals (gPN ≥ 0.85), optical and microphysical properties~~coefficients are calculated from the following ~~equations~~equation:

$$Ext = \frac{\pi}{4}\sum_i \beta_{ext}^i N_i D_i^2 \qquad (1)$$

where β^i_{ext} is the extinction efficiency (values depend on spherical or aspherical particle characterization), D_i the mean diameter in channel i, and N_i the number concentration.

Different approaches are used to retrieve ice water content from spherical and non-spherical particles (Garret et al., 2003 ; Gayet et al., 2004 ; Gayet et al., 2012). For spherical particles (gPN > 0.85), IWC is computed from the following equation:

$$IWC_{spherical} = \frac{\pi}{6}\rho_{ice}\sum_i N_i D_i^3 \qquad (2)$$

~~where β^i_{ext} is the extinction efficiency (depending on spherical or aspherical particle characterization), D_i the mean diameter in channel i, N_i the number concentration, and~~with ρ_{ice} the bulk ice density (0.917 g cm^{-3}).

For non-spherical ice crystals (gPN < 0.85 and for particle diameters larger than 70 µm), an equivalent diameter method is used (Gayet et al., 2004). For an ice crystal with an area A, the particle equivalent diameter D_{equ} (in mm for eq. (3) and (4)), the equivalent mass x_{equ} (in mg), and the Ice Water Content (IWC in mg m^{-3}) are defined as~~-~~:

-A ≤ 0.049 mm² $$D_{equ} = \sout{0}0.82\text{-}A^{0.48} \quad (3)$$

-A > 0.049 mm² $$D_{equ} = 0.56\text{-}A^{0.32} \quad (4)$$

$$x_{equ} = \frac{\pi}{6}\rho_{water}{D_{equ}}^{3} \quad (5)$$

$$IWC_{non-spherical} = \sout{\rho_{ice}\sum_{i} N_i x_{equ}\rho_{water}} \sum_{i} N_i x_{equ} \quad (6)$$

with ρ_{water} the bulk water density (1 g cm^{-3}).

These equations do not account for possible shattering of large ice crystals on the probe inlets. This effect is minimized in young contrails but can lead to an overestimation of small ice crystal concentration in contrail cirrus clouds.

Trace gas measurements were also performed. NO/NO_y concentrations can be significant in young tropospheric aircraft plumes~~, the main chemical component to be measured is NO_y, mainly composed of NO and NO_2. During CONCERT campaigns trace gas measurements of~~. NO and NO_y mixing ratio were performed using the chemiluminescence technique (Schlager et al., 1997) with a time resolution of 1 s. Instruments used for CONCERT campaigns are described in several studies (Jurkat et al., 2010 ; Jurkat et al., 2011 ; Voigt et al., 2014 ; Jurkat et al., 2016). The accuracy (and precision) of the NO and NO_y measurements are estimated with 7% (and 10%) and 10% (and 15%), respectively (Ziereis et al., 2000).

~~Chemical ionization mass spectrometry combined with a SF_5^- ion source was used to detect the concentration of HNO_3, SO_2, and HONO in the exhaust plumes and the UTLS (Jurkat et al., 2010, Jurkat et al., 2011). Mass spectra were sampled with an ion trap mass spectrometer with resolution of < 0.3 atomic mass units and averaged over five spectra resulting in an overall time resolution of 1.6 s. Detection limits for HONO and SO_2 for 1.6 s time resolution were 72 and 67 pmol mol^{-1} and for HNO_3 36 pmol mol^{-1} for 32 s time resolution. During CONCERT 2011 a quadrupole mass spectrometer was employed on the Falcon (Voigt et al., 2014) with detection limits of 15 pmol mol^{-1} for HNO_3 and 8 pmol mol^{-1} for SO_2 at 20 s time resolution (Jurkat et al., 2016).~~

~~The detection of water vapor and~~ Relative humidity with respect to ice (RHI) is ~~important~~also key parameter to ~~characterize~~understand contrail ~~ice crystals.~~formation and microphysical properties. Water ~~vapor has been~~vapour was measured with the chemical ionization mass spectrometer AIMS-H2O during CONCERT-2 (Kaufmann et al., 2014; 2016). ~~In addition,~~ Hygrometers using the Lyman-~~α~~-α technique (FISH, Zöger et al., 1999; Meyer et al., 2015), and frost point hygrometers (CR-2, Heller et al., 2017) were ~~implemented~~deployed on the Falcon during CONCERT-1 and 2.

3 Results

3.1 Overview of the cloud properties sampled during the reference cases

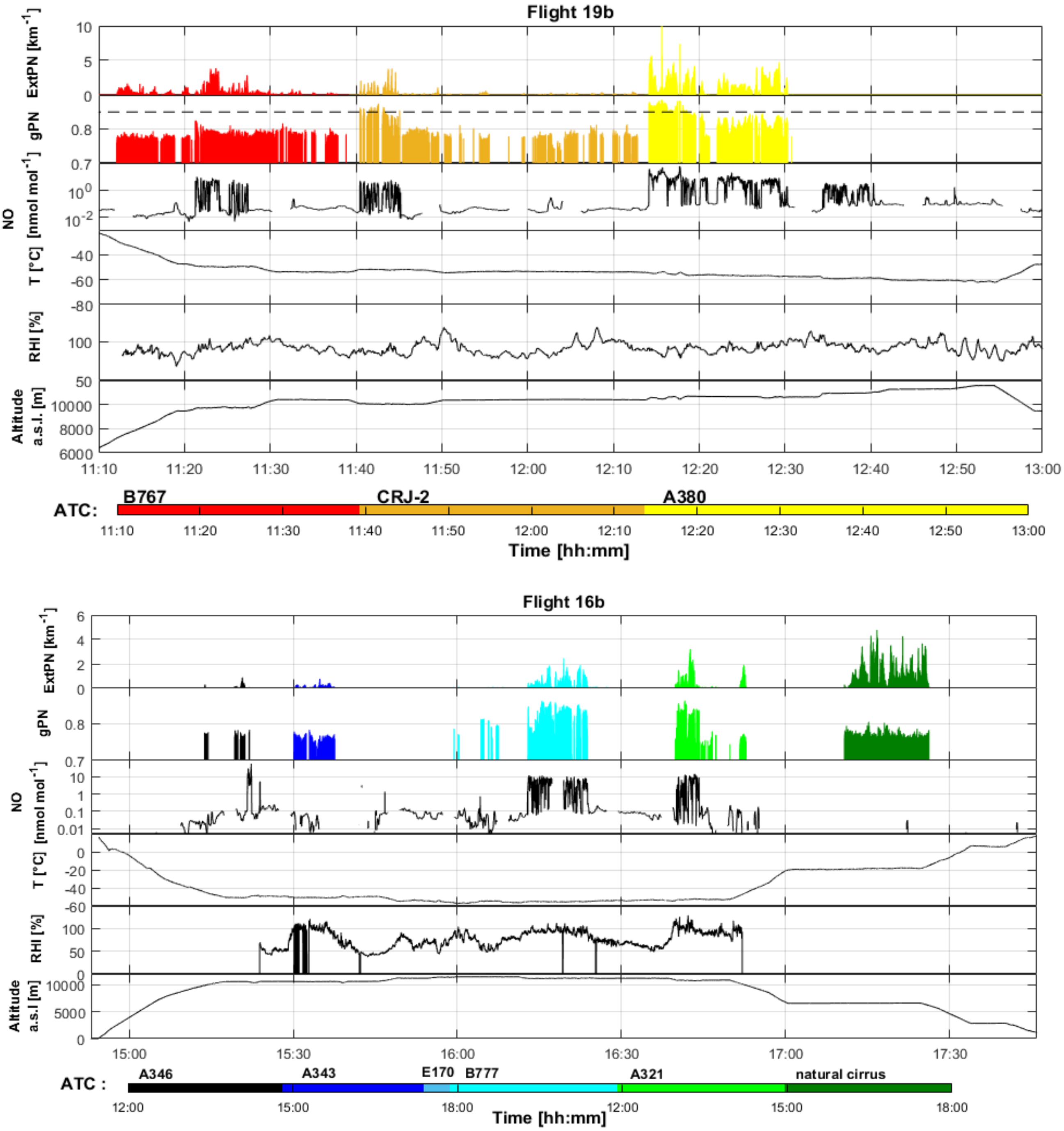

Figure 1: Time series at 1 s resolution for flights a) 19b (CONCERT 1) and b) 16b (CONCERT 2). From top to bottom: extinction coefficient (in km^{-1}) and asymmetry parameter measured by the Polar nephelometer at 804 nm (dashed line corresponds to a 0.85 value), concentration of nitric oxide (in nmol mol^{-1}) measured by chemiluminescence technique, temperature (in °C), relative humidity with respect to ice (in %), and altitude a.s.l. (in m). Temporal series are coloured according to time and aircraft chasing information from Air Traffic Control (ATC).

The purpose of this section is to give an overview of the contrail optical properties and more interestingly to evaluate the ability of the Polar Nephelometer measurements to identify contrails. Two flights, performed on 16 September 2011 during CONCERT-2 (flight 16b) and on 19 November 2008 during CONCERT-1 (flight 19b), respectively, were selected for their variety of contrails and cirrus sampled during these two flights. The two flights are considered as a benchmark to illustrate the potential of the PCA methodology described in Sect. 3.2.

Figure 1 displays the time series of the extinction coefficient (ExtPN) at 804 nm,and the asymmetry parameter (gPN) at a wavelength of 804 nm, relative humidity with respect to ice (RHI), and the nitric oxide (NO) concentration, the temperature T and the altitude for flights 19b and 16b. RHI measured with the AIMS mass spectrometer is shown for flight 16b. For RHI measurements onduring flight 19b we refer to as well as instrument shortcomings are discussed in details in Kübbeler et al. (2011);), Gayet et al. (2012);), Jessberger et al. (2013) ;and Schumann et al. (2013). For both flights, Air Traffic Control (ATC) providedprovides information on the flight tracks and on the chased aircraft characteristics (aircraft type, engine type, fuel flow, weight, engine power setting,…) responsible for the formation of encountered contrails. In a first classification approach, the). Form this information the Falcon measurements were attributed to the exhaust plume of individual aircraft with an estimated plume age. Time series are colorcolour coded according to the ATC information of consecutive sampling of different contrails. .

The PN extinction coefficient coupled with the asymmetry parameter seems to be a reasonable proxy to detect contrails and cirrus clouds (see amongst other references, Voigt et al., 2010). ExtPN values, by definition, depend on the cloud particle concentration and size. Values typically beyond 0.1 km^{-1} correspond in general to cloud events that are well correlated to supersaturationenvironmental conditions supersaturated with respect to ice conditions (RHI > 100%). Figure 1 provesshows that relatively high values of extinction can be found in flights 19b and 16b whichthat are linked to the presence of contrails or cirrus clouds. Moreover, the temporal distributions of these values are coherentin accordance with ATC information for both flights. For instance, most of the contrails induced by commercial aircraft exhaust plumes translate intoare associated with significant extinction coefficient values. The ExtPN values are between 0.2 km^{-1} and 10 km^{-1} for contrails induced by A346, A340, and A380 commercial aircraft. Cirrus clouds are detected with more variable extinction values mostly larger than 0.5 km^{-1}. Most of the aircraft induced contrails are detected by the PN with the exception ofexcept for the ones stemming from the E170 airplane. At 15:50 during flight 16b, ATC identified the E170 position close to the Falcon flight trajectory, however the ExtPN and the NO mixing ratio remained very low. Hence, the E170 contrail was not probed by the Falcon. In the following we assume that only periods with ExtPN values above 0.1 km^{-1} are considered as a reasonably reliable signature forof contrails sampled during the flight campaigns.

The absolute values of the asymmetry parameter gPN provide additional information ofon the cloud particle shape. Indeed, gPN is a good indicator of the degree of sphericity of ice crystals (Gayet et al., 2012). Ice clouds with gPN values higher or equal to 0.85 are typically composed of spherical ice crystals, whereas lower values are indicative of aspherical ice particles. In a supersaturated environment of contrails, crystals grow by water vaporvapour deposition and become increasingly aspherical with time. This is whyHowever, in very young contrails, spherical ice crystals prevail in very young contrails with an asymmetry coefficient around 0.85 with RHI above 100%. Subsequently,prevail. gPN is decreasing when water vaporvapour diffusion is generating more and more aspherical crystal shapes at ice supersaturation. This can be observed for A321 chasing during flight 16b withwhere gPN is decreasing to a value of 0.75 whilst RHI remains around 100%, whereas for %. This is not the case during B777 chasing, where no gPN decrease is observed atwhen RHI < 80%. Also 100%. However, it is important to note that the RHI measurements during the CRJ-2 chasing events do not show supersaturated conditions, whereas contrail seems persistent. Indeed, RHI measurements should be discussed carefully for this campaign due to calibration issues.

Natural cirrus clouds are mainly composed of non-spherical ice crystals, possibly with hexagonal shapes. These clouds can be easily discriminated from young contrails as they exhibit a much lower asymmetry parameter typically below 0.75 (see amongst others Jourdan et al., 2003b, Febvre et al., 2009). However, no accurate ambient RHI data can be retrieved for measurements in natural cirrus due to instrumental calibration problems. A good example of the evolution of gPN is the CRJ-2 contrail observed between 11:40 and 11:45 during flight 19b. The sequence illustrates the potential of the gPN measurement to characterize the evolution of contrail properties~~, with decreasing crystal sphericity documented by the decreasing~~. The evolution of the ice crystal shape is reflected in the decrease of the asymmetry parameter from 0.88 to 0.79 (uncertainties around 0.04) after only 5 min and down to 0.77 after 20 min. A ~~more stable variation~~ weaker decrease of gPN values (around 0.78 ± 0.02) is then observed until 12:10 ~~after~~corresponding to 30 min of contrail ageing ~~associated with crystal growth~~. During this period, ice crystals are expected to grow by water ~~vapor~~vapour diffusion. A similar decrease ~~in~~of gPN values has been ~~noted~~reported by Gayet et al. (2012) in the ageing contrail from an A380 aircraft, and is also visible in the present study for the B767 and the A321 contrails.

NO concentration measurements can also be used to discriminate natural cirrus clouds from ice clouds influenced by aircraft traffic. At the typical altitude of 10 km, NO environmental concentrations are close to background values. In contrast, NO concentrations in young contrails may reach several tens of nmol mol^{-1} (Voigt et al., 2010). Figure 1 shows a good correlation between the expected localization of young contrails and NO concentrations. The dilution effect ~~into~~in the upper troposphere causes an important decay of chemical concentrations. For instance, the first few seconds of the A380 chasing during flight 19b are characterized by a high NO concentration (up to 40 nmol mol^{-1}) followed by a fast decrease to 10 nmol mol^{-1} in the next 15 min, and less than 5 nmol mol^{-1} beyond 15 min. NO concentrations finally decrease to background levels within hours (e.g. Voigt et al., 2017). This decrease of the NO concentration is in accordance with the decrease of the extinction coefficient (from 10 to 0.2 km^{-1}) and asymmetry parameter (from 0.88 to 0.77). ~~Thus~~ NO ~~was~~is mainly used as an additional contrail indicator. However, during some aircraft chasing events, NO concentrations were near background levels, while mass spectrometric measurements (not shown here) indicate elevated concentrations of HONO, HNO_3, and SO_2 representative for contrail chemical species.

~~The above case studies of~~ Flights 19b and 16b clearly show that the optical properties of contrail ~~type ice~~ clouds (supported by the ATC information) in conjunction with specific trace gas concentration measurements can be used to discriminate contrails from natural ice cloud events. A first order analysis of these parameters can be used to roughly distinguish young contrails (mostly quasi-spherical ice crystals) from aged contrails (mostly aspherical ice crystals) and natural cirrus (background NO concentrations). This analysis is mainly qualitative and based solely on a few ~~integrated~~typical parameters (Fig. 1). A more robust statistical method should be used to accurately separate the different contrail phases ~~and also~~from natural cirrus. In the following section, relationships between contrail and ice cloud properties ~~and their~~ scattering properties are investigated more extensively to assess whether the information content of the PN scattering measurements is sufficient to document changes in the contrail microphysical properties.

3.2 Statistical Method

In this section, we present a methodology based on the statistical analysis of the optical signature of ~~ice clouds and in particular~~ contrails and cirrus. The goal is to classify the contrail properties according to the aircraft origin and evolution stage. The main objective of the Principal Component Analysis (PCA) is data reduction ~~in order~~ to allow a better physical interpretation of the light scattering patterns derived from the Polar Nephelometer measurements (Legendre and Legendre, 1998; Jourdan et al., 2003). In this study, optical properties of ice crystals in the evolving contrail environment are ~~analyzed~~examined to evaluate contrail evolution. This statistical analysis was already successfully applied to discriminate mixed phase clouds (Jourdan et al., 2003 ; Jourdan et al., 2010~~),~~) from liquid clouds~~,~~ and ice clouds, ~~(Jourdan et al., 2003) as well as~~and to ~~characterize~~identify porous aerosol in degassing plumes (Shcherbakov et al., 2016~~) using light scattering properties measured by the Polar Nephelometer.~~).

3.2.1 Reference definition

The PCA is first applied to the PN angular scattering coefficients measurements performed during flights 16b and 19b which are here considered as our reference ~~datasets~~dataset. Initially, a correlation matrix is calculated to characterize the link between each scattering angle. The PCA is designed to generate a new limited set of uncorrelated parameters, called principal components C_{lj} representative of the original data set variability.

A first implementation of the PCA is performed to detect unreliable data or out of order photodiodes. For instance, seven photodiodes presented a low signal to noise ratio and were excluded from the dataset. Flight sequences characterized by ExtPN<0.1 were also removed. Finally, flight sequences dedicated to aircraft chasing and ice cloud sampling were considered to perform a second PCA.

~~Then,~~ The analysis is performed on the remaining angular scattering coefficients (4669 Angular Scattering Coefficients (ASC) representing PN measurements of flights 16b and 19b) ~~now~~ restricted to 25 angles θ ranging from 15° to 155°. The new set of variables or coordinates, C_{lj}, can be expressed with the scalar product of the vector of reduced angular scattering coefficients ~~-~~$\overrightarrow{\sigma_j}(\theta)$ for the j^{th} measurements, expressed in log scale, and the l^{th} eigenvector $\xi_l(\theta)$ (i.e. principal component) of the total data set correlation matrix (Jourdan et al., 2010).

$$C_{lj} = (\overrightarrow{\ln \sigma_j} - \langle \overrightarrow{\ln \sigma} \rangle)^T . \overrightarrow{\xi_l} \quad (4)$$

where $\langle \overrightarrow{ln\sigma} \rangle$ represents the average ASC of the dataset.

The first three eigenvectors $\overrightarrow{\xi_l(\theta)}$ ~~-~~of the correlation matrix are displayed in Fig. 2 along with their normalized eigenvalues λ_l, representing more than 99% of the variability of the PN angular scattering coefficients (ASC).

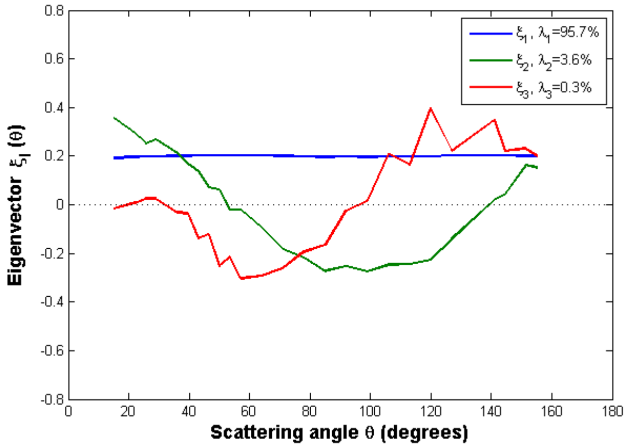

Figure 2: First three eigenvectors for the flights 16b and 19b.

The first eigenvector $\xi_1(\theta)$ is approximately constant versus scattering angle and represents 95.7% of the total variance. It means that this principal component is representative of changes of the magnitude of phase functions without any changes in their global shape. This ~~behavior~~behaviour means that 95.7% of the ASC variations are linked to changes of the cloud particle extinction. Results show a good correlation ($r^2 = 0.98$) between the first eigenvector and the extinction derived from the PN measurements (ExtPN).

The second eigenvector ξ_2~~(θ)~~ (θ)reverses sign twice at scattering angles equal to 50° and 140° with an extremum around 90°. Accordingly, 3.6% of the angular scattering variability corresponds to a redistribution of scattered energy from the angular region (50°-140°) to scattering angles lower than 50° and higher than 140°. Light-scattering ~~modeling~~modelling studies demonstrate that the scattering ~~behavior~~behaviour in the angular region between 60° and 140° is sensitive to the particle shape and thermodynamic phase (Jourdan et al., 2010). A strong linear correlation ($r^2=0.97$) between the second eigenvector and the asymmetry coefficient (gPN) at 804 nm is found.

The third eigenvector represents only 0.3% of the total variance. However, this eigenvector

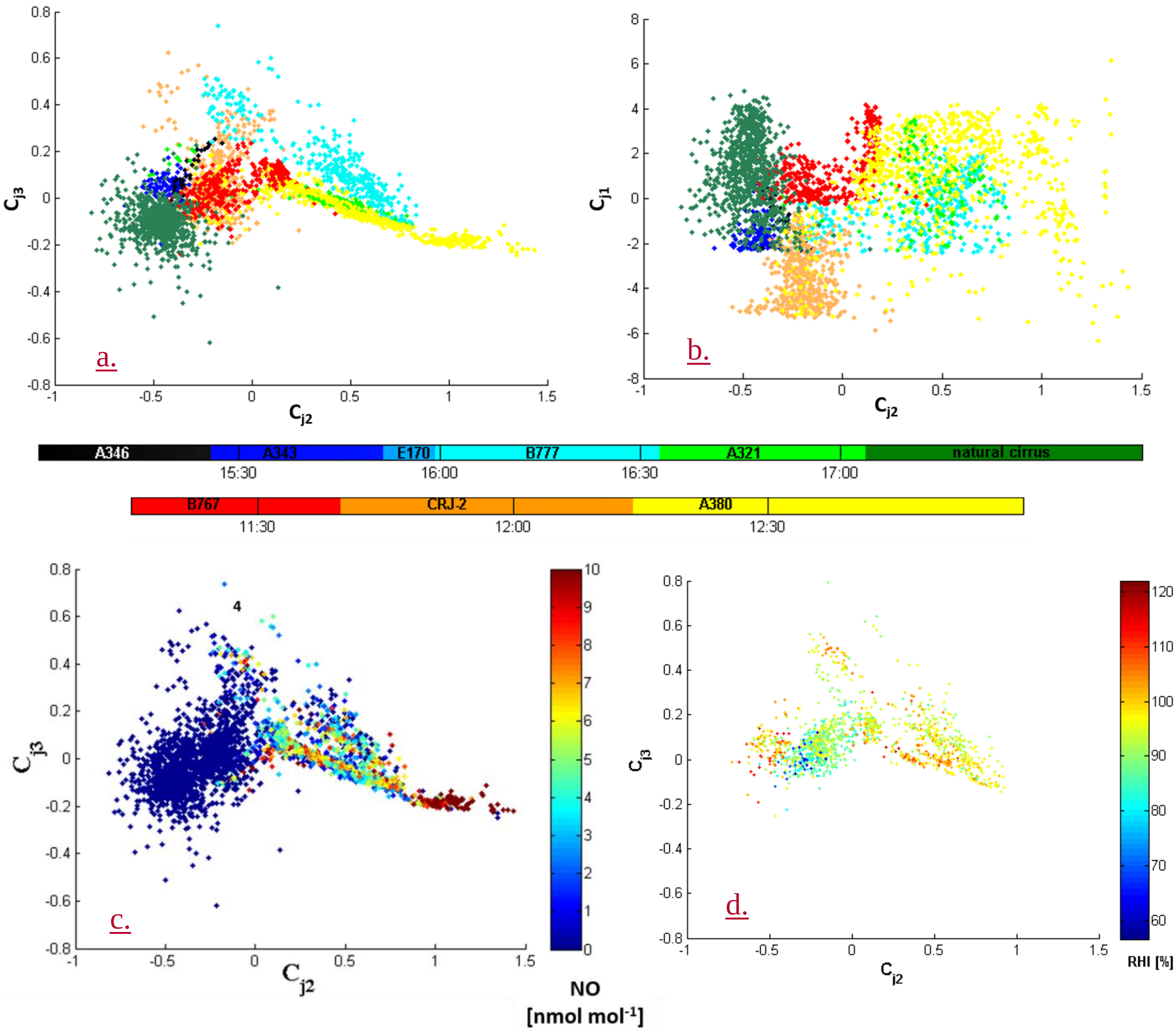

Figure 3: Expansion coefficient diagram for flights 16b and 19b: third versus second principal component for a), c) and d), and first versus second principal component for b). Data points are colour coded according to ATC information for a) and b), by NO concentration for c), and by RHI values for d).

provides additional information in scattering regions which are not well described by the first two principal components. It has opposite signs in the angular region (30°-90°) and (90°-155°) with maximum extremal values at 60° and 120°. The shape of the third eigenvector describes the forward/backward hemisphere partitioning of the scattering. Baran et al. (2012), Xie et al. (2006), and Xie et al. (2009) showed that the scatter pattern for angles between 120° and 160°, corresponding to ice bow-like effects, is sensitive to quasi-spherical particles. Moreover, these backscattering angles (θ>120°) and scattering angles around 22° and 46° (corresponding to halo features) can also be linked to the particle habits and surface roughness (Xie et al., 2009, Jourdan et al., 2010).

~~Based on these three first principal components,~~ Each phase function (or ASC) measured by the PN can be expressed with a good accuracy as a linear combination of ~~these~~the three principal components (Jourdan et al., 2010). The PN data are projected into a new space defined by the three principal components (3D-space) instead of the 25-dimensional space of ASC. The scatterplots of the C_{j3} and C_{j1} expansion coefficients versus the C_{j2} coefficient are represented on Fig. 3a and b respectively. Fig. 3a illustrates the features of the ASC measurements in one of the most comprehensive way. Each point corresponds to a measured phase function documented over 25 angles. The variability of C_{j2} coefficients is significant with values ranging from -1 to 1.5. The angular variation of the second principal component indicates that large values of C_{j2} (C_{j2} > 0.75) correspond to ASC with low side scattering (60°-130°) and higher forward scattering (15°-40°) and somehow higher backscattering (145-155°). This ~~behavior~~behaviour is connected to an increase of the asymmetry parameter with an increase of C_{j2} values. Thus, the fraction of spherical particles increases with increasing C_{j2}. In the region defined by negative values of C_{j2} the density of points is relatively high. These cloud events exhibit optical properties characterized by a large side scattering and low asymmetry parameter. Therefore, specific cloud sequences sharing similar scattering properties can be identified based on this second principal component. Young contrails characterized by quasi-spherical ice crystals have high positive values of C_{j2} while cirrus clouds and contrail cirrus exhibit high negative values.

In the space of the third principal component high positive values of C_{j3} imply that less energy is scattering in the forward hemisphere and thus more energy is scattered in the backward hemisphere. The variability of the expansion coefficients is less pronounced as ASC are distributed between -0.4 and 0.6. Most of the measured ASC do not significantly differ from the average ASC in the angular ranges (30°-90°) and (90°-155°). However, some specific clusters linked to scattering ~~behavior~~behaviour can be identified for values of C_{j3} greater than 0.1 and lower than -0.1. These threshold values also depend of the position of the ASC on the second principal component. Finally, the first principal component is directly linked to the extinction coefficient. High values of C_{j1} are representative of optically dense cloud sequences.

~~Based on the time series displayed in Fig. 1, data points corresponding to contrails are also color coded according to their aircraft origin illustrated on Fig. 3a and b. From these information and based on the first three principal components, 6 clusters (see numbered ellipsoids in Fig. 3) representative of particular scattering behavior can be roughly identified. Figure 3a suggests an increase of C_{j2} and a decrease of C_{j1} with increasing aircraft size. Figure 3c shows an increase of C_{j2} for increasing NO mixing ratio. Some contrails or ice cloud events are clearly delimited by a single area in the C_{j3} versus C_{j2} and also C_{j2} versus C_{j1} diagrams. For instance cirrus clouds are gathered in cluster 5. Most of the contrails induced by the B767, A340 and CRJ2 aircraft are associated to cluster 3 or 5. It means that these cloud events share similar optical properties characterized by a low asymmetry parameter, high side scattering behavior, and supersaturated ambient conditions with respect to ice. More interestingly, Fig. 3 shows that some contrail events are smeared out over several areas or clusters.~~Figure 3c shows an increase of C_{j2} for increasing NO mixing ratio. ~~Contrails relative to the A380 aircraft are dispatched in cluster 0 and 2 while the ones corresponding to the B777 are spread out between clusters 1 and 4.~~ This clearly indicates that the contrails are evolving in space and/or time along the Falcon flight track~~ while chasing the respective contrails. This evolution can also be seen in the in-situ measurements of NO concentration color coded on Fig. 3c.~~. Cloud regions influenced by air traffic can be discriminated from clouds formed by natural processes based on the NO concentration values. ~~While clusters 3 and 5 are characterized by very low NO concentrations (close to zero) above background, clusters 0, 1, 2, and 4 correspond to higher concentrations representative of a significant aircraft exhaust influence. For instance, a clear trend shows that an increase of NO concentration translates into higher values of C_{j2}.~~ Hence, contrails characterized by a low side scattering due to the presence of spherical ice crystals correspond to high NO concentration. This ~~behavior~~behaviour can be a signature of young contrail properties. Elder or aged contrails composed of a higher fraction of non-spherical crystals or growing more aspherically are expected to exhibit an enhanced side scattering and a lower asymmetry parameter associated to lower NO concentrations. RHI measurements also give relevant information on the capacity of the cloud to be persistent. Thus, Fig. 3d shows higher RHI values with decreasing gPN values.

3.2.2 Clustering analyses

The new representation of each measurement in the space of the first three principal component reveals different clusters, characteristic of specific scattering behaviour. The clustering k-mean method (Seber 1984, Spath 1985) is applied to the reference dataset (fights 19b and 16b) to partition the observations into k clusters to minimize the variance within each cluster (i.e. to minimize the distance between each data point and the centre of the cluster it belongs to). The number of cluster k is an adjustable parameter. Then in a first step, each observation is assigned to a specific cluster whose mean has the least squared Euclidean distance (i.e. nearest mean). In a second step, the position of each cluster is set to the mean of all data points belonging to that cluster (i.e. the centroids of each of the k clusters becomes the new means). These two steps are repeated until convergence is reached when the assignments no longer change.

16 clusters were found to encompass all points of the two flights and to partition each aircraft chasings identified from ATC information (Fig. 3a and 3b). For clarity and better understanding of the variability of contrail properties, we choose to limit the number of clusters to 6. 9 clusters are merged into 2 clusters to define the group “natural-cirrus” and B767 / A343 / CRJ-2 contrails (referred hereafter to Cluster 3 and 5 respectively). 4 clusters are also gathered in one new cluster corresponding to A321 / A380 contrails (referred to Cluster 2 hereafter). In addition, only data within the 10% of the maximum Mahalanobis distance (De Maesschalck et al., 2000) to the respective cluster’s centre has been considered for this analysis.

Clusters are defined by their means (or centres), standard deviations (or widths), and cross-correlations (or tilts). The Mahalanobis distance is given by the equation:

$$D_M(x)_i = \sqrt{(x - \mu_i)^T S_i^{-1} (x - \mu_i)} \quad (5)$$

with D_M the Mahalanobis distance between point χ and the i[th] cluster center, μ_i the N-dimensional mean of this cluster and S_i its covariance matrix.

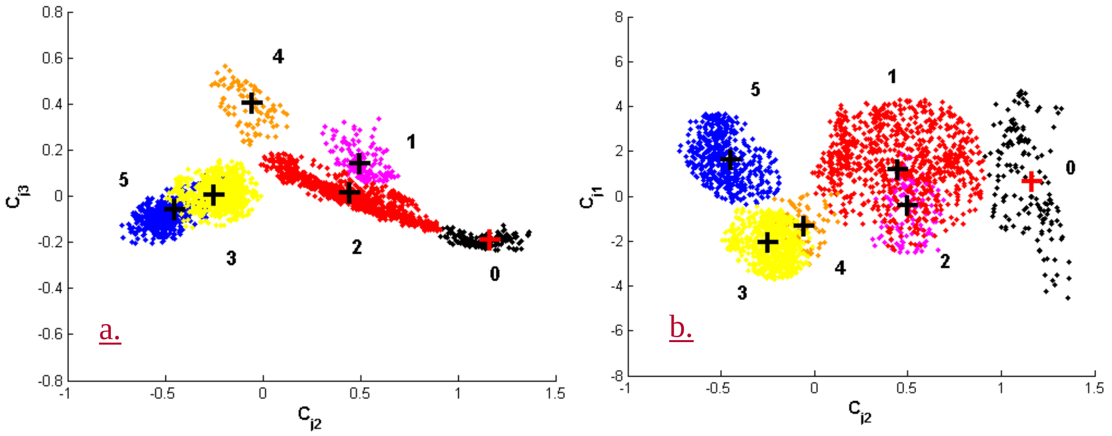

Figure 4: Clustering results of the k-mean method applied to the base (flights 16b and 19b). Third versus second principal component for a), and first versus second principal component for b). Only data within the 10% of the maximum Mahalanobis distance to the respective cluster's centers have been considered for this analyse.

Figure 4 shows the partitioning of the dataset into the 6 new clusters (clusters 0 to 5). In the following we use data from chemical tracers and optical measurements, and aircraft type information to support and discuss the results of the k-means clustering method.

While clusters 3 and 5 are characterized by very low NO concentrations (close to zero, Fig. 3c) above background, clusters 0, 1, 2, and 4 correspond to higher concentrations representative of a significant aircraft exhaust influence. ATC information shows that cirrus clouds are gathered in cluster 5. Most of the contrails induced by the B767, A343, A346 and CRJ2 aircraft are associated to cluster 3 or 5. These cloud events share similar optical properties characterized by a low asymmetry parameter, high side scattering behaviour, and supersaturated ambient conditions with respect to ice for some cases. Contrails relative to the A380 aircraft are dispatched in cluster 0 and 2 while the ones corresponding to the B777 are spread out between clusters 1 and 4.

The contrail and cirrus classification based on ASC measurements appears to be consistent with the independent trace gas measurements. Each cluster represented on Fig. ~~3~~4 can be linked to a distinct cloud event. Therefore, the combination of flights 16b and 19b can provide a relevant test-bed database to discriminate contrail properties. Young contrails (spherical ice crystals) are associated to clusters 0, 1 or 2, whereas aged contrails (aspherical ice crystals and ~~higher~~high RHI values) with more pristine ice are categorized in clusters 3 and 4, and finally natural cirrus (low NO concentrations) are found in cluster 5. A less precise analysis (using onboard camera) reveals that cluster 0 corresponds essentially to the primary wake created below the secondary wake behind an aircraft. ~~These different clusters are defined arbitrarily according to ATC information and according to their optical differences through the three first principal components. In the following, the clusters will be referenced according to the contrail evolution stage~~ Table 1 summarizes these cluster's definitions and names used in this work.

- ~~Cluster 0 : Primary Wake (PW)~~
- ~~Cluster 1 : Young Contrail 1 (YC1)~~
- ~~Cluster 2 : Young Contrail 2 (YC2)~~
- ~~Cluster 3 : Aged Contrail Clean (ACC)~~

~~- Cluster 4 : Aged Contrail (AC)~~
~~- Cluster 5 : Cirrus Cloud (CC).~~

~~Thus, the next step is to validate these cluster definitions according to the different tracers. One has to~~

Cluster number	definition	name
0	Primary Wake	**PW**
1	Young Contrail 1	**YC1**
2	Young Contrail 2	**YC2**
3	Aged Contrail 1	**AC1**
4	Aged Contrail 2	**AC2**
5	Cirrus Cloud	**CC**

Table 1: Cluster's definitions according to ATC information and tracer measurements (NO concentrations and RHI values)

One should keep in mind that some points are still arbitrarily attributed to a particular cluster without strong physical justification.

3.2.~~2 Application to~~3 Merging other CONCERT flights

In this section we ~~investigate the possibility to~~ complement the previous analysis with additional cloud optical measurements performed during other CONCERT flights to increase the robustness of the method.

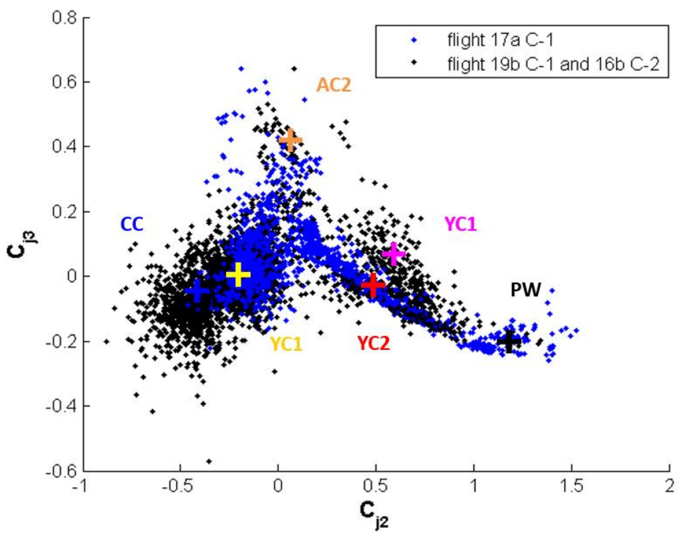

Figure 5: Example of data projection in the C_{j2}/C_{j3} space where data from flight 17a (blue data points) are superposed on the data from the benchmark flights 19b and 16b (black data points).

~~The principal components obtained on the basis of the measurements performed during flight 16b and 19b are considered as our reference axes. Now,~~ The ASC measured during other flights can be projected ~~on this~~in the space of the principal components established with flights 16b and 19b dataset. The coordinates of ~~these~~ the data points corresponding to the other flights are calculated from Eq. (4). An example of this data projection is illustrated in Fig. ~~4~~5 where flight 17a is represented in the C_{j2}/C_{j3} space. ~~Every PCA~~Each data point can be attributed to one cluster previously defined by the ~~PCA~~

~~implemented with~~k-mean clustering method based on flights 16b and 19b ~~data~~dataset (black points). In other words, ~~every~~the ASC measured during another flight can be merged (projected) into the expansion coefficient diagram ~~relative to the base measurements performed during flights 16b and 19b.~~displayed on Fig. 3. Data points sharing similar optical properties will ~~still~~ be close to each other~~. According to the cluster definition, Fig. 4~~ on such plot. Figure 5 shows that different contrail phases ~~have been experienced~~are observed during flight 17a. Data points are mostly grouped into cluster ~~ACC~~AC1, but are also present in clusters ~~AC~~AC2, YC2, and PW. Finally, cloud data ~~encountered~~gathered during this flight are mainly categorized as young and aged contrails.

We follow this methodology to project and classify each additional "contrail" ~~flight~~event performed during both CONCERT campaigns~~. In order to attribuate each measurement (or point) to one cluster and to enhance the statistical significance of our clustering analysis we compute the~~ with minimum Mahalanobis distance (~~De Maesschalck et al., 2000). Clusters are defined by their means (or centers), standard deviations (or widths), and cross-correlations (or tilts).~~ see Eq. (5)).

			Cluster							
			PW	YC1	YC2	AC1	AC2	CC	Number of points	Age (s)
			1st wake	young contrails		aged contrails		Cirrus		
Day / Aitcraft	17a C-1	TOTAL							1435	
		A340-311							359	61 - 144
	17b C-1	TOTAL							2715	
		B737-500							310	77 - 151
		A340-642							100	82 - 139
		NC							189	-
	19a C-1	TOTAL							2152	
		A319-111							628	94 - 129
		A340-311							175	63 - 90
	19b C-1	TOTAL							1647	
		B767-300							319	77 - 107
		CRJ-2							151	80 - 95
		A380-841							677	109 - 240
	20 C-1	TOTAL							1434	
		B737-300							64	90 - 290
	16b C-2	TOTAL							1511	
		A340-600							128	100 - 132
		B777							378	120 - 160
		A321							135	70 - 95
	17 C-2	TOTAL							2904	
		NC1							498	-
		NC2							233	-
	24 C-2	TOTAL							1380	
		B777							371	112 - 178

Table 2: Classification relative to the six clusters on the Cj2/Cj3 representation of the PCA of all data points for each flight of the two CONCERT campaigns (C-1 in November 2008 and C-2 in September 2011). The legend of the bars represents the relative contribution of data points of individual contrails (blue bars) and also entire flights (black bars) to the 6 individual clusters.

The ~~Mahalanobis distance is given by~~ assignment of the ~~equation:~~

$$D_M(x)_i = \sqrt{(x-\mu_i)^T S_i^{-1}(x-\mu_i)} \quad (5)$$

~~with D_M the Mahalanobis distance between point χ and the i^th cluster center, μ_i the N-dimensional mean of this cluster and S_i its covariance matrix. Each~~ data ~~point can be associated to a specific cluster corresponding to the shorter Mahalanobis distance, and the ellipsoids' eccentricity and width can be adjusted.~~

~~The classification relative~~points to the six clusters shown on the ~~C_{j3} vs C_{j2} and the C_{j1} and C_{j2}~~ expansion diagrams is summarized in Table ~~1. A total of~~2. 8 flights (6 additional flights) representing 4426 ASC measurements ~~was~~were processed. The lengths of the bars in Table ~~1~~2 represent the ~~relative contributions~~distribution of the data points ~~to~~within the different clusters: a) black ~~bar merge cloud data points~~ bars correspond to the fraction of cloud events within a specific flight (with extinction coefficient higher than 0.1 km^{-1}) ~~for entire flights~~ and b) blue bars ~~present~~ represent cases of individual ~~aircraft~~ contrails within ~~specific flights. An important fraction (at least~~the flight. Data points with extinction coefficient lower than 0.1 km^{-1} are not shown in the table. More than 30~~%)~~% of the data points ~~is detected~~are located in clusters ~~ACC~~AC1 and/or CC ~~for each flight during the two campaigns. This indicates~~meaning that ~~these data points are sampled in~~they correspond to aged contrail and sometimes natural cirrus. ~~For flights more~~Flights clearly performed in well visible contrails outside natural cirrus (earlier development stage and/or intensified persistent elder contrails~~),~~) exhibit significant ~~fractions~~fraction of data points ~~are~~ associated to clusters PW, YC1, and YC2 (young contrails) for both CONCERT-1 and CONCERT-2 campaigns. However, within these flights ~~are also characterized by a significant contribution of~~ data points ~~to~~are also gathered in cluster ~~ACC~~AC1 (aged contrails clean) and to a ~~minor~~lesser extent in cluster ~~AC~~AC2 (aged contrails, mostly corresponding to measurements performed during two different B777 contrail chasing events).

These results are in reasonable agreement with previous conclusions (this subsection) ~~about~~drawn for the cluster definitions and associated contrail / ice cloud characteristics. Very young contrails have been mostly chased during CONCERT-1 (flights 19a~~, 19b~~ and ~~20) and during CONCERT-2 (flights 16b, 17 and 24).~~19b). Another interesting result is related to flight 17 during CONCERT-2 (flight 17 C-2~~). No contrail~~) where no aircraft information ~~has been communicated from~~was provided by ATC~~, however~~. Still ATC data indicate measurements in exhaust plumes and the Falcon ~~has been flying~~flew apparently in visible contrails~~,~~ (ExtPN > 0.1 km^{-1}) which were probably too old for ATC recognition. Our analysis shows that these data points can mainly be attributed to cluster CC~~, and to a minor extent to cluster ACC and cluster YC2.~~ and AC1. This observation suggests that significantly aged contrails have been sampled~~, resembling strikingly natural cirrus clouds. Indeed~~. However, crystal formation and growth processes in contrails and natural cirrus suggest that very old contrails more and more resemble natural cirrus properties. ~~From Table 1 it is obvious that an important amount of data points had been sampled in natural cirrus during this flight. All these natural cirrus data points appear in the black bars but only to a minor extent in the blue bars limited to ATC communicated contrail sequences.~~

ATC information on ~~contrail~~exhaust plume ages ~~has been~~was also collected during each chasing. Some chasings ~~have been~~were performed less than 100 s after contrail formation. This is the case for the A340 contrail during flight 19a and for the CRJ-2 contrail during flight 19b of CONCERT-1 and for the A321 contrail during flight 16b of CONCERT-2. One can notice that the contrail ages are well correlated to the chosen cluster definitions, revealing that contrail data relative to the A340 are included in cluster ~~YC1~~PW and YC2 (young contrails) for more than ~~53~~90% of the data points, and nearly ~~65~~63% for the CRJ-2 and ~~88~~84% for the A321. According to our cluster classification, only ~~12~~5% of the data points gathered during these three flights correspond to aged contrail (cluster ~~ACC~~AC1 and ~~AC~~AC2) categories in contrast to other ~~–~~CONCERT-1 and CONCERT-2 flights (with more than 30% of data points associated to ~~ACC~~AC1 and ~~AC~~AC2). Even though it is still difficult to associate contrail ages to measurement points, the "contrail age" ranges ~~are in agreement~~agree with the cluster definitions.

4 Evolution of contrail properties

4.1 Optical and chemical cluster properties

~~As demonstrated~~ In the previous ~~part,~~section we showed that cloud events can be separated according to their light-scattering properties. Six clusters were defined based on two flights ~~with~~having a significant number of data points ~~for~~distributed in each cluster. In this section we present the mean optical, chemical, and microphysical properties for each ~~of the six clusters. These mean~~cluster. The average properties ~~have been~~are calculated ~~over~~for all data points associated to the 6 individual clusters (all flights, both CONCERT campaigns). ~~Figure 5a, 5c~~Figures 6a, 6c, and ~~5d illustrate~~6d show the normalized frequency distributions of the asymmetry parameter (gPN), the extinction coefficient (ExtPN), and NO concentrations for the six clusters, respectively. Figure ~~5b~~6b represents the mean normalized scattering phase functions~~, also for the 6~~ of each clusters. However, it should be noted that the number of data points could differ significantly from one cluster to another (from 141 measurements for Cluster YC1 to 8950 measurements for Cluster AC1).

The asymmetry parameter gPN statistics ~~for the six clusters~~ shown in Fig. ~~5a~~6a provide the most ~~relevant information on cloud characteristics and the related context~~striking evidence of the relationship between contrail evolution~~/age.~~ stage and optical properties. In agreement with findings ~~in~~of Gayet et al. (2012), aged contrails (cluster ~~ACC~~AC1 and ~~AC~~AC2) and natural cirrus (cluster CC) correspond to gPN values ~~between~~ranging from 0.72 ~~and~~to 0.80~~,~~. Younger contrails (cluster YC1 and YC2) ~~to~~ have values of gPN ~~between~~of 0.80 ~~and~~to 0.86~~, and~~. Values of the asymmetry parameter in the primary wake ~~measurements~~ (cluster PW) ~~to gPN~~are typically above 0.86. ~~This result can be explained with~~These features are a consequence of the time evolution of ice crystal shapes ~~after exhaust~~ from quasi-spherical ice particle after exhaust to~~,~~ non-spherical (e.g. column, needle, bullet, and bullet-rosette type crystals~~.~~) as the contrail evolves. In the primary wake, the pressure increases ~~associated~~ in the descending vortex. This leads to adiabatic heating and subsequent sublimation ~~processes~~ of the ice crystals (Lewellen and Lewellen, 2001; Unterstrasser et al., 2016) ~~and explains a return to~~that can explain the spherical shapes ~~and~~of ice crystals and thus, the high values of the asymmetry coefficients.

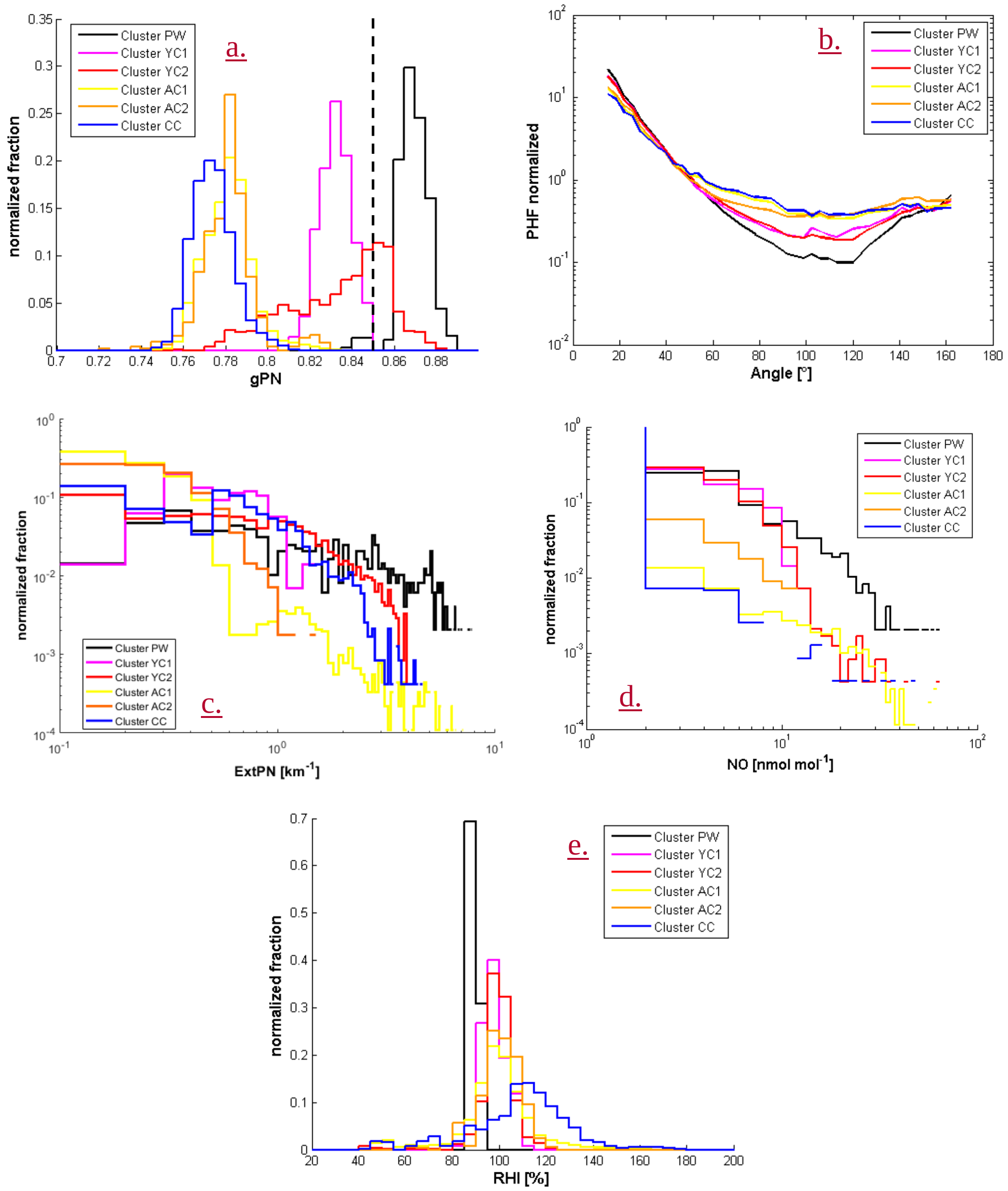

Figure 6: Normalized histograms of a) asymmetry coefficient (dashed line corresponds to a value of 0.85), b) phase function, c) extinction retrieved by Polar Nephelometer, d) NO concentration for all flights, and e) RHI conditions for CONCERT-2 flights.

The normalized phase functions are presented in Fig. ~~5b~~6b. Primary wake phase functions (cluster PW) are clearly different from the young contrail phase functions (cluster YC1 and YC2), which are themselves different from aged contrails (cluster ~~ACC~~AC1 and ~~AC~~AC2) and natural cirrus (cluster CC) phase functions. The main difference ~~between the averaged phase functions~~ is observed ~~for~~in the side scattering region (50°-140~~°) which~~°). This region is related to changes of ice particles shapes and to the ~~proportion~~fraction of spherical ice crystals within the contrails. This ~~behavior~~behaviour is expected and ~~also in agreement~~agrees with the position of ~~cluster~~clusters PW, YC2 and YC1 on the expansion coefficient diagram (Fig. 2). Indeed, the decrease of the C_{j2} coefficient is associated to a side scattering enhancement. Therefore, very young contrails are composed ~~of a majority~~mainly of spherical ice crystals ~~are characterized by~~ for which the phase functions ~~with~~indicate a substantial scattering at forward angles ~~associated with~~and much lower scattering at sideward angles. As the contrails evolve, these features smooth out leading to phase functions with a featureless ~~behavior and a more~~ flat ~~appearance~~behaviour at side scattering angles. Finally, the averaged normalized phase functions of old contrails and natural cirrus are ~~resembling~~similar to each other. This also explains that they are difficult to discriminate ~~with~~within the PCA.

The extinction coefficient statistics are presented in Fig. ~~5c~~6c. All the aged contrails (cluster ~~ACC~~AC1 and ~~AC~~AC2) exhibit extinction coefficients lower than 2 km^{-1}. ~~The same statement applies for~~Also 80% of the sampled natural cirrus (cluster CC~~).~~) show such low extinction coefficients. For younger contrails (cluster YC1 and YC2~~)~~), the extinction coefficients can reach 5 km^{-1}. Largest extinction coefficients are ~~achieved~~found in primary wake measurements ~~sorted into~~ (cluster PW) with ~~extinction coefficients reaching~~ values up to 8 km^{-1}. Still, the main fraction (more than 50% of data points) of young contrail data yields extinction coefficients ~~between~~from 0 ~~and~~to 1 km^{-1}.

Concentrations of chemical species can also ~~allow characterizing~~be used to characterize contrail/cirrus ~~cloud data~~properties. The concentration depends strongly on the type of the ~~pursued~~tracked aircraft. Figure ~~5d~~6d shows the mean ~~concentrations~~concentration of nitrogen oxide NO ~~data points attributed to~~ for the six individual clusters. Young contrail NO concentrations (cluster PW, YC1 and YC2) can reach values up to 10 nmol mol^{-1} ~~and up~~(corresponding to 10% of measurements). For primary wake measurements (PW in black) a higher concentration can be reached. Approximately 1% of the data have concentrations close to 60 nmol mol^{-1} in the primary wake. In contrast, in aged contrails and in natural cirrus (cluster ~~ACC, AC~~AC1, AC2 and CC) NO concentrations higher than 2 nmol mol^{-1} do not exceed ~~10 nmol mol^{-1} (which is true for more than 97.5%, 99.6%, and 99.7~~1% of ~~data points for clusters ACC, AC, and CC, respectively).~~cases. Indeed, after exhaust, concentrations of nitrogen oxide NO and ~~sulfur~~sulphur dioxide SO_2 created by combustion reactions decrease rapidly due to the dispersion in the upper troposphere and reactions with other molecules.

Finally, saturation conditions with respect to ice are presented in Fig. ~~5e~~6e for all clusters ~~and for CONCERT-2 flights only.~~. The predominant measured ambient relative humidity ~~in~~of all clusters is around 95%. Cluster ~~ACC~~AC1 and CC (yellow and blue ~~and red~~ lines~~) show~~ respectively) exhibit median RHI values close to 110% and 120% respectively. These higher ~~RHI values (more than 120%) than other clusters. Thus, this can explain~~ values are suitable for the persistence of the contrail and the formation of ~~natural~~ cirrus ~~and persistent contrails for these ambient~~clouds Supersaturated conditions~~. Contrary to all other clusters, no supersaturation is observed for cluster PW (in black), defined as~~ are not reached for the measurements gathered in the primary wake ~~measurements. This result is in agreement with the definition of the primary wake, which is still in the non-persistent phase of the contrail~~cluster (PW). Low humidity values may well occur in primary wakes with non-persisting contrails.

~~The above~~These results highlight that the principal component analysis, based on the ASC measurements described in Sect. 3, ~~allows~~can be used to discriminate ~~different types of contrails.~~contrail phases. Specific optical and chemical properties can thus be ~~characterized~~derived for each contrail phase and can be related to their evolution~~. An interesting aspect is that the PCA analysis facilitates to connect clusters of optical properties to microphysical characteristics of the contrails within specific clusters~~.

4.2 Microphysical cluster properties

Microphysical properties are assessed using the combination of FSSP-300 and 2DC measurements~~. They have been analyzed for each cluster for~~ or hydrometeor diameters ~~between~~ranging from 0.5 µm ~~and~~to 800 µm~~.~~, but with a gap in the size range 17 µm to 70 µm. Figure

67 shows mean volume the averaged number particle size distributions (PSD) for each cluster and for all six clusters measured from the FSSP-300 and 2DC with respective limited instrumental size ranges. flights of the study (8 flights from CONCERT-1 and 2). A linear interpolation in logarithmic space has beenis applied for each PSD in the size range from 17 µm to 70 µmto cover the gap from 17 µm to 70 µm. Because of this gap, the derived microphysical properties should be considered with caution, but may be used to check the cluster definitions.

PSD measurements in natural cirrus and aged contrails differ significantly depending on the location of the study, ambient air conditions, measurement methods (instrument limitation (Gayet et al., 2002), and air speed (Febvre et al., 2009)). Previous studies show that a 3-hours old contrail cirrus with an effective diameter close to 20 µm (Voigt et al., 2017) and number concentration larger than 0.1cm^{-3} (Schumann et al., 2017) can be composed of ice crystals with sizes up to 100 µm (blue dashed line, contrail cirrus figure 7). This differs from the PSD of the natural cirrus presented by Voigt et al. (2017) (dashed black line), which is not accurately documented by the two instruments. These results include all flights of the study (8 flights from CONCERT-1 and 2). It is important to note that more than 500 data points are included in each cluster with a maximum of 6300 data points for cluster ACC.has an order of magnitude lower particle number concentration. In natural cirrus at mid-latitudes, ice crystals with size up to 1600 µm were observed during the ML-CIRRUS campaign (dark dashed line Figure 7, Voigt et al., 2017).

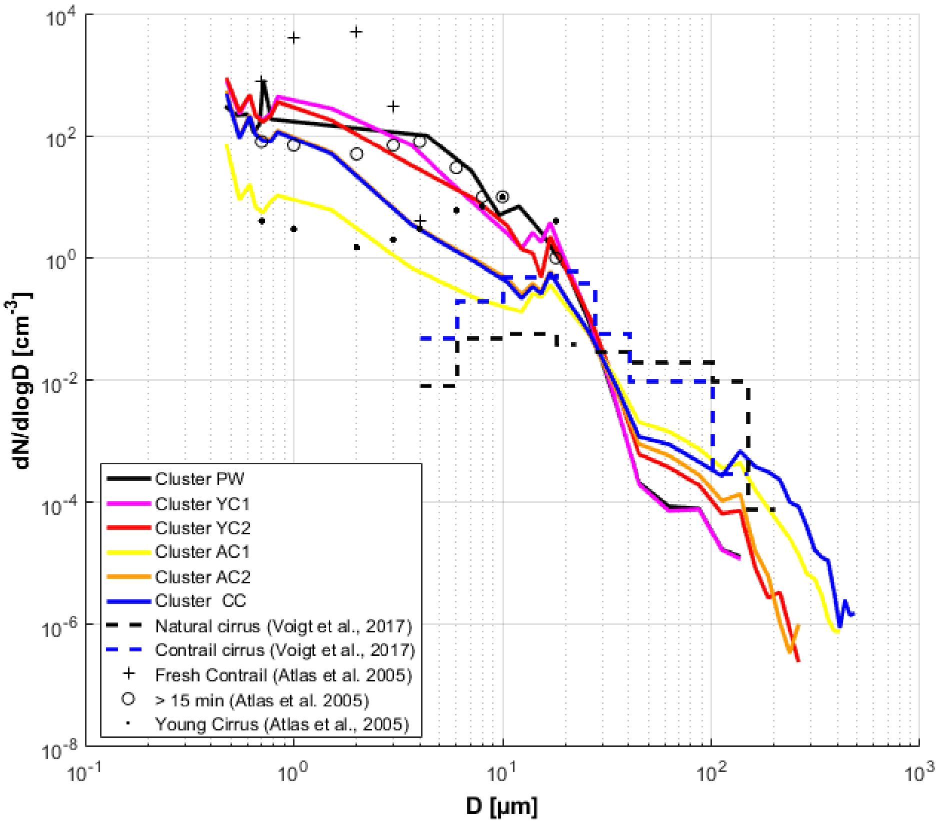

Figure 7: Number particle size distribution for each cluster including all data points of all flights. FSSP-300 measurements from 0.5 to 17 µm and 2DC measurements from 70 µm to 800 µm. The data are linearly interpolated in logarithm space between 17 µm and 70 µm.

Figure 67 shows that the mean number PSDs forof each cluster are consistent with the cluster definition and these previous studies. Indeed, two categories of PSD can be observed. Within the FSSP-300 size range, PSD relative to old contrails (cluster ACCAC1 and ACAC2) and cirrus (cluster

CC) exhibit more than number concentration of small ice particles one order of magnitude lower number concentrations of small ice crystal compared to than young contrails (clusterclusters YC1 and YC2) and primary wake (cluster PW). Within the two groups, no significant differences can Differences in this size range should be noticedcarefully considered due to uncertainties of the FSSP-300 number concentration measurements of , which is close to 30% for typical concentrations aroundof 5cm^{-3} and but can reach 75% for concentrations aroundof approximately 0.5 cm^{-3} (Gayet et al., 2002). However, we can still discriminate primary wake measurements (cluster PW) from secondary wake measurements (clusters YC1 and YC2) in the 3 to 10 µm size range. In addition, it is interesting to note that aged contrail measurements classified into AC1 cluster present significantly lower ice particle concentrations than natural cirrus. The differences observed between these two groups can beenthe PSD of PW/YC1/YC2 and AC1/AC2/CC can be explained by the production of small ice crystals (from 1 to 10 µm) in fresh exhaust plumes followed by rapid dilution during subsequent minutes after the exhaust.

Within the 2DC range, the PSDs are also in agreement with the cluster definitions. A higher concentration of large ice crystals with diameters around 100 µm and beyondlarger are expected for natural cirrus (cluster CC) and for significantly well-developed contrails. This is particularly well illustrated onby the mean PSD from cluster YC1 that displays significantly less particles in the 2D-C2DC measurements size range where a higher concentration of large ice crystal is observed for clusters ACCthan the one corresponding to AC1 and CC compared to the younger contrails. However, these PSD do not allow discriminating young contrails in primary wake (cluster PW) from contrails in the secondary wake (cluster YC1 and YC2).AC2.

Extinction (km^{-1})		Mean	std	Median	percentile 25	percentile 75
cluster	PW	4,230	3,820	3,308	1,104	6,485
	YC1	0,720	0,410	0,680	0,351	1,026
	YC2	2,070	2,655	1,017	0,271	2,836
	AC1	0,220	0,484	0,037	0,008	0,158
	AC2	0,110	0,161	0,054	0,004	0,126
	CC	0,370	1,240	0,046	0,001	0,132

IWC (mg m^{-3})		Mean	std	Median	percentile 25	percentile 75
cluster	PW	8,173	10,586	5,573	1,665	11,363
	YC1	0,191	0,107	0,168	0,111	0,281
	YC2	4,860	8,918	1,235	0,218	6,604
	AC1	7,072	35,765	0,124	0,000	1,151
	AC2	0,295	1,079	0,094	0,003	0,286
	CC	27,929	144,384	0,126	0,005	0,448

NTOTAL (cm^{-3})		Mean	std	Median	percentile 25	percentile 75
cluster	PW	172,965	114,497	152,398	95,564	223,374
	YC1	409,726	205,625	405,127	230,907	603,187
	YC2	188,139	199,736	125,344	52,584	236,100
	AC1	8,206	6,550	1,696	0,966	3,363
	AC2	28,883	43,758	9,176	2,954	42,626
	CC	5,092	24,453	3,444	1,467	6,511

Table 3: Optical and microphysical properties for each cluster according interpolated particle size distributions from FSSP-300 and 2DC measurements.

Table 23 presents ice water content (IWC, in mg m^{-3}) and total number of ice crystals (NTOTAL, in particles cm^{-3}) derived from the measured PSD for each cluster. The extinction coefficient (in km^{-1}) obtained from the PN measurements is also displayed. Despite the large uncertainties associated to both instruments and the interpolation ~~method (for ice crystals with diameters ranging from 17 µm and 70 µm), these results again prove that each cluster can be connected to specific contrail phases. The microphysical and optical properties of cluster PW are in agreement with the cloud properties excepted in the primary wakes. The extinction coefficient has a mean value of 3.9 km^{-1}, IWC is close to 15.5 mg m^{-3}, and the number concentration yields a typical value of 125 particles cm^{-3}. Young (clusters YC1 and YC2) and aged contrails (clusters ACC and AC) exhibit distinctive differences in their optical and microphysical properties. Higher extinction coefficients and ice number concentration, 2 km^{-1} and 160 cm^{-3}, respectively, characterize young contrails compared to aged contrails with 0.08 km^{-1} and 10 particles cm^{-3}, respectively. Cluster CC corresponds to natural cirrus clouds where significant atmospheric spreading and ice growth occurred. Thus, within this cluster the extinction coefficients (mean values of 0.1 km^{-1}) as well as the number concentration of ice crystals (around 6 particles cm^{-3}) are very low. The IWC is higher with a mean value of 28.7 mg m^{-3} due to ice crystal growth in supersaturated conditions~~between 17 µm and 70 µm diameters, these results again show that each cluster can be connected to a specific contrail phase, and their properties can be compared to previous studies.

~~However, it is difficult to discriminate young contrail cases (YC1 and YC2) based on their microphysical properties. Clusters ACC and AC microphysical properties are also similar but ACC IWC and number concentrations are closer to the ones of the cirrus case indicating a more evolved stage of the observed ACC contrail cluster.~~

In terms of cluster mean values, the microphysical and optical properties of cluster PW agree with the cloud properties expected in the primary wakes. The extinction coefficient has a mean value of 4.23 km^{-1}, IWC is close to 28 mg m^{-3}, and the number concentration yields a typical value of 173 particles cm^{-3}. These properties are in agreement with previous measurement reported by Gayet et al. (2012) with particle number concentrations close to 200 cm^{-3} for contrails less than 60 s after their formation. Their work also reports extinction coefficient around 7 km^{-1} presenting the highest values of the contrail life time.

Young (clusters YC1 and YC2) and aged contrails (clusters AC1 and AC2) exhibit distinctive differences in their extinction coefficients and their concentrations of ice particles. Higher extinction coefficients and ice number concentration, more than 0.7 km^{-1} and 170 cm^{-3}, respectively, characterize young contrails compared to aged contrails, with less than 0.4 km^{-1} and around 10 particles cm^{-3}, respectively. The ice number concentrations are in agreement with previous results with values between 200 and 100 cm^{-3} for contrail ages between 60 s and 3 min, and around 5 cm^{-3} for contrail ages around 10 min (Goodman et al., 1998 ; Lawson et al., 1998 ; Schröder et al., 2000 ; Schäuble et al., 2009 ; Gayet et al., 2012 ; Voigt et al., 2017). The IWC values differ significantly between clusters YC1 and YC2 which may be due to a lower number of large particles with diameter higher than 20 µm in YC1 than in YC2. Cluster CC corresponds to natural cirrus clouds which experienced strongly variable spreading and ice growth. Indeed, the IWC is significantly higher (28 mg m^{-3}) within this cluster than in other clusters. However, the ice number concentration and the extinction coefficient are higher than in previous studies, with values around 0.1 cm^{-3} and 0.023 km^{-1} respectively. Besides to interpolation between the FSSP-300 and the 2DC measurements, the assumed shape (spherical or aspherical), and shattering of large ice particles in cirrus and aged contrails can also have a significant effect on the measurement of optical and microphysical properties (Gayet et al., 2012).

Conclusions

In this study, a new form of statistical analysis of contrail to cirrus evolution is presented based on two intensive contrail measurement campaigns, CONCERT-1 and CONCERT-2. The data are used to study optical and microphysical properties of contrails during their evolution from young contrails to contrail-cirrus clouds, and of ambient natural cirrus clouds. The combination of optical, microphysical, ~~and~~ chemical airborne ~~measurement data~~ measurements with aircraft chasing information from ATC was used to ~~present~~provide an extended view of cloud properties~~, and to merge those results with ATC flight information about sampled contrails~~.

A Principal Component Analysis (PCA) methodology ~~has been~~was applied to the measured Polar Nephelometer scattering phase function data ~~in order~~ to facilitate ~~a distinction between~~the discrimination of cloud properties ~~in~~of different contrail phases. The PCA results were derived first for two reference flights that sampled contrails and cirrus in various development stages, including the primary wake, the young secondary wake, old contrails (few minutes after formation) and natural cirrus. For these flights, the PCA clearly demonstrates ~~the~~its potential to ~~separate~~discriminate different groups of clouds, justifying the use of these two flights as a benchmark. Thereafter, the scattering phase functions measured during other CONCERT flights were ~~then~~ projected into the space of principal components obtained from the two reference flights. ~~Mahalanobis distances were used to measure the separation between the additional~~Individual data points ~~and the data in~~ were assigned to the predefined ~~clusters.~~cluster with minimum Mahalanobis distances. From the entire data set, the cloud properties in the various contrail development stages can be ~~separated and analyzed~~analysed separately.

The analysis demonstrates that the clearest separation between clusters is ~~related to~~derived from particle shape, which ~~is significantly controlling~~impacts the scattering phase function and the derived asymmetry parameter gPN. The asymmetry parameter clearly separates young contrails (gPN of 0.72 to 0.80) from contrail/cirrus with gPN ranging from 0.80 to 0.88. Since ~~it is still difficult to evaluate~~ the exact contrail age ~~of each measurement~~was not always known, young and aged contrails are classified also by their optical and chemical properties. The measured NO concentrations are also useful to distinguish natural cirrus from old contrails.

Despite the ~~important~~large size gap between the size ranges of the two instruments used ~~to measure particle size distributions~~, particle size spectra and related mean values of the ice particle number concentration, extinction and ice water content have been determined for each cluster. The various clusters clearly show different size distributions. In good agreement with previous findings on optical and chemical properties, we find that young contrails have more than a factor of ten higher number concentrations of small ice crystals (with diameters lower than 20 µm) than aged contrails and natural cirrus. On the other hand, aged contrails and natural cirrus contain larger ice crystals, with diameters larger than 75 µm. The optical and microphysical properties of the aged contrail cirrus are often similar to those found in the ambient "natural" cirrus clouds. The results show that the PCA method allows to identify and discriminate different contrail growth stages and to provide an independent method for the characterization of the evolution of contrail properties.

In agreement with Shcherbakov et al. (2016), who characterised volcanic and cirrus using optical measurements, the PCA method has been clearly shown here to be suitable for contrail studies. The additional use of microphysical and chemical measurements can be added to the PCA method in order to improve the selection of contrail phases. Different ranges of extinction or asymmetric coefficients could be also used for PCA analyses in this perspective. However, additional parameters should be carefully selected to limit the bias introduced by the limitations of the probes and the optimal selection may vary from one measurement campaign to another.

Accurate ~~modeling~~modelling of cirrus or contrails' single scattering properties is ~~a primary condition~~required for the interpretation of remote sensing measurements. Therefore, measurements of the optical characteristics of ice crystals in natural conditions are still needed for validation of numerical techniques and for the determination of free parameters in light scattering models. In this context, the results from the PCA could be used to develop representative parameterizations of the scattering ~~and geometrical~~ properties ~~of~~and the ice crystals' shapes and sizes observed in the visible wavelength range~~ that then have to be extrapolated into the near infrared~~.

Acknowledgments

We thank ~~financing~~for financial support by the Helmholtz Association under contract VH-NG-309 and W2/W3-60. Part of this work was funded by DFG SPP HALO 1294 contract VO1504/4-1, and by the DLR project Eco2Fly in ML-CIRRUS-cirrus special issue. We thank Lufthansa, the DLR flight department and ~~DFS~~the Deutsche Flugsicherung for excellent support during the campaign. The in-situ data can be found in the HALO-database (https://halo-db.pa.op.dlr.de/).

References

Baran, A.J., Gayet, J.-F., and Shcherbakov, V.: On the interpretation of an unusual in-situ measured ice crystal scattering phase function. Atmospheric Chemistry and Physics 12, 9355–9364, 2012.

Baumgardner, D., Dye, J.E., Gandrud, B.W., and Knollenberg, R.G.: Interpretation of measurements made by the forward scattering spectrometer probe (FSSP-300) during the Airborne Arctic Stratospheric Expedition. Journal of Geophysical Research 97, 8035–8046, 1992.

Borrmann, S., Luo, B., and Mishchenko, M.; Application of the T-Matrix Method to the Measurement of Aspherical (Ellipsoidal) Particles with Forward Scattering Optical Particle Counters. Journal of Aerosol Science 31, no. 7 (2000): 789–799, 2000.

Burkhardt, U., Kärcher, B., and Schumann, U.: Global modeling of the contrail and contrail cirrus climate impact. Bulletin of the American Meteorological Society 91, 479–484, 2010.

Burkhardt, U. and Kärcher, B.: Global radiative forcing from contrail cirrus. Nature Climate Change, 1(1), 54–58, 2011.

Carleton, A.M., Silva, A.D., Aghazarian, M.S., Bernhardt, J., Travis, D.J., and Allard, J.: Mid-season climate diagnostics of jet contrail "outbreaks" and implications for eastern US sky-cover trends. Climate Research, 56, 209–230, 2013.

Chen, C.-C. and Gettelman, A.: Simulated 2050 aviation radiative forcing from contrails and aerosols. Atmospheric Chemistry and Physics, 16(11), 7317–7333, 2016.

Duda, D. P., Minnis, P., Khlopenkov, K., Chee, T.L., and Boeke, R.: Estimation of 2006 Northern Hemisphere Contrail Coverage Using MODIS Data. Geophysical Research Letters, 40, 612-617, doi:10.1002/grl.50097, 2013.

Febvre, G., Gayet, J.-F., Minikin, A., Schlager, H., Shcherbakov, V., Jourdan, O., Busen, R., Fiebig, M., Kärcher, B., and Schumann, U.: On optical and microphysical characteristics of contrails and cirrus. Journal of Geophysical Research: Atmospheres (1984–2012) 114, 2009.

Frömming, C., Ponater, M., Dahlmann, K., Grewe, V., Lee, D.S., and Sausen, R.: Aviation-induced radiative forcing and surface temperature change in dependency of the emission altitude. Journal of Geophysical Research: Atmospheres (1984–2012) 117, 2012.

Gayet, J. F., Gayet, J.F., Crépel, O., Fournol, J.F., and Oshchepkov, S.: A new airborne Polar Nephelometer for the measurements of optical and microphysical cloud properties. Part I: Theoretical design. In Annales Geophysicae, pp. 451–459, 1997.

Gayet, J.-F., Auriol, F., Minikin, A., Ström, J., Seifert, M., Krejci, R., Petzold, A., Febvre, G., and Schumann, U.: Quantitative Measurement of the Microphysical and Optical Properties of Cirrus Clouds with Four Different in Situ Probes: Evidence of Small Ice Crystals. Geophysical Research Letters 29, no. 24: 2230. doi:10.1029/2001GL014342, 2002.

Gayet, J.-F., Gayet, J.F., Crépel, O., Fournol, J.F., and Oshchepkov, S.: A new airborne Polar Nephelometer for the measurements of optical and microphysical cloud properties. Part I: Theoretical design. In Annales Geophysicae, pp. 451–459, 1997.

Gayet, J.-F., Ovarlez J., Shcherbakov, V., Ström, J., Schumann, U., Minikin, A., Auriol, F., Petzold, A., and Monier M.: Cirrus Cloud Microphysical and Optical Properties at Southern and Northern Midlatitudes during the INCA Experiment. Journal of Geophysical Research: Atmospheres 109, no. D20 : D20206. doi:10.1029/2004JD004803, 2004.

Gayet, J.-F., Shcherbakov, V., Voigt, C., Schumann, U., Schäuble, D., Jeßberger, P., Petzold, A., Minikin, A., Schlager, H., Dubovik, O., and Lapyonok, T.: The evolution of microphysical and optical properties of an A380 contrail in the vortex phase. Atmospheric Chemistry and Physics. 12, 6629–6643, 2012.

Garrett, T.J., Gerber, H., Baumgardner, D.G., Twohy, C.H., and Weinstock, E.M.: Small, highly reflective ice crystals in low-latitude cirrus. Geophysical Research Letters 30, 2132, 2003.

Gettelman, A., and Chen, C.: The climate impact of aviation aerosols. Geophysical Research Letters, 40, 2785–2789, doi:10.1002/grl.50520, 2013.

Gierens, K. and Dilger, F.: A climatology of formation conditions for aerodynamic contrails, Atmospheric Chemistry and Physics, 13, 10847-10857, doi:10.5194/acp-13-10847-2013, 2013.

Graf, K., Schumann, U., Mannstein, H., and Mayer, B.: Aviation induced diurnal North Atlantic cirrus cover cycle. Geophysical Research Letters 39, L16804, doi:10.1029/2012GL052590, 2012.

Goodman, J., Pueschel, R.F., Jensen, E.J., Verma, S., Ferry, G.V., Howard, S.D., Kinne, S.A., and Baumgardner, D.: Shape and size of contrails ice particles. Geophysical Research Letters 25, 1327–1330, 1998.

Heller, R., Voigt, C., Beaton, S., Dörnbrack, A., Kaufmann, S., Schlager, H., Wagner, J., Young, K., and Rapp, M.: Mountain waves modulate the water vapor distribution in the UTLS, Atmospheric Chemistry and Physics, Discussion, doi:10.5194/acp-2017-334, in review.

Heymsfield, A., Baumgardner, D., DeMott, P., Forster, P., Gierens, K., and Kärcher, B.: Contrail Microphysics. Bulletin of the American Meteorological Society 91, 465–472, 2010.

Heymsfield, A.J., and Parrish, J.L.: A computational technique for increasing the effective sampling volume of the PMS two-dimensional particle size spectrometer. Journal of Applied Meteorology 17, 1566–1572, 1978.

Heymsfield, A., Baumgardner, D., DeMott, P., Forster, P., Gierens, K., and Kärcher, B.: Contrail Microphysics. Bulletin of the American Meteorological Society 91, 465–472, 2010.

Irvine, E.A., Hoskins, B.J., and Shine, K.P.: The dependence of contrail formation on the weather pattern and altitude in the North Atlantic. Geophysical Research Letters 39, L12802, doi:10.1029/2012GL051909, 2012.

Järvinen, E., Schnaiter, M., Mioche, G., Jourdan, O., Shcherbakov, V.N., Costa, A., Afchine, A., Krämer, M., Heidelberg, F., Jurkat, T., Voigt, C., Schlager, H., Nichman, L., Gallagher, M., Hirst, E., Schmitt, C., Bansemer, A., Heymsfield, A., Lawson, P., Tricoli, U., Pfeilsticker, K., Vochezer, P., Möhler, O., and Leisner, T.: Quasi-spherical Ice in Convective Clouds, Journal of Atmospheric Sciences, doi:10.1175/JAS-D-15-0365.1, 2016.

Jansen, J. and Heymsfield, A. J.: Microphysics of aerodynamic contrail formation processes, Journal of Atmospheric Sciences, 72(9), 3293–3308, 2015.

Jeßberger, P., Voigt, C., Schumann, U., Sölch, I., Schlager, H., Kaufmann, S., Petzold, A., Schäuble, D., and Gayet, J.F.: Aircraft type influence on contrail properties, Atmospheric Chemistry and Physics, 13, 11965-11984, doi:10.5194/acp-13-11965-2013, 2013.

Jourdan, O., Oshchepkov, S., Gayet, J.-F., Shcherbakov, V., and Isaka, H.: Statistical analysis of cloud light scattering and microphysical properties obtained from airborne measurements. Journal of Geophysical Research 108, 4155, 2003.

Jourdan, O., Mioche, G., Garrett, T.J., Schwarzenböck, A., Vidot, J., Xie, Y., Shcherbakov, V., Yang, P., and Gayet, J.-F.: Coupling of the microphysical and optical properties of an Arctic nimbostratus cloud during the ASTAR 2004 experiment: Implications for light-scattering modeling. Journal of Geophysical Research: Atmospheres (1984–2012) 115, 2010.

~~Jourdan, O., Oshchepkov, S., Gayet, J.-F., Shcherbakov, V., and Isaka, H.: Statistical analysis of cloud light scattering and microphysical properties obtained from airborne measurements. Journal of Geophysical Research 108, 4155, 2003.~~

~~Jurkat, T., Kaufmann, S., Voigt, C., Schäuble, D., Jeßberger, P., and Ziereis, H.: The airborne mass spectrometer AIMS – Part 2: Measurements of trace gases with stratospheric or tropospheric origin in the UTLS, Atmospheric Measurement Technics, 9, 1907–1923, doi:10.5194/amt-9-1907-2016, 2016.~~

Jurkat, T., Voigt, C., Arnold, F., Schlager, H., Aufmhoff, H., Schmale, J., Schneider, J., Lichtenstern, M., and Dörnbrack, A.: Airborne stratospheric ITCIMS-measurements of SO_2, HCl, and HNO_3 in the aged plume of volcano Kasatochi, Journal of Geophysical Research, 115, D00L17, doi:10.1029/2010JD013890, 2010.

Jurkat, T., Voigt, C., Arnold, F., Schlager, H., Kleffmann, J., Aufmhoff, H., Schäuble, D., Schäfer, M., and Schumann, U.: Measurements of HONO, NO, NOy and SO2 in aircraft exhaust plumes at cruise, Geophysical Research Letters, 38, L10807, doi:10.1029/2011GL046884, 2011.

Jurkat, T., Kaufmann, S., Voigt, C., Schäuble, D., Jeßberger, P., and Ziereis, H.: The airborne mass spectrometer AIMS – Part 2: Measurements of trace gases with stratospheric or tropospheric origin in the UTLS, Atmospheric Measurement Technics, 9, 1907–1923, doi:10.5194/amt-9-1907-2016, 2016.

Kärcher, B., and Voigt, C.: Formation of nitric acid/water ice particles in cirrus clouds, Geophysical Research Letters, 33, L08806, doi:10.1029/ 2006GL025927, 2006.

Kärcher, B., and Voigt, C.: Susceptibility of contrail ice crystal numbers to aircraft soot particle emissions, Geophysical Research Letters, 44, 8037-8046, doi:10.1002/2017GL074949, 2017.

Kärcher, B., and Yu, F.: Role of aircraft soot emissions in contrail formation. Geophysical Research Letters, 36, L01804, doi:10.1029/2008GL036649, 2009.

Kaufmann, S., Voigt, C., Jeßberger, P., Jurkat, T., Schlager, H., Schwarzenboeck, A., Klingebiel, M., and Thornberry, T.: In situ measurements of ice saturation in young contrails, Geophysical Research Letters, 41, doi:10.1002/2013GL058276, 2014.

Kaufmann, S., Voigt, C., Jurkat, T., Thornberry, T., Fahey, D. W., Gao, R.-S., Schlage, R., Schäuble, D., and Zöger, M.: The airborne mass spectrometer AIMS – Part 1: AIMS-H_2O for UTLS water vapor measurements, Atmospheric Measurement Technics, 9, 939-953, doi:10.5194/amt-9-939-2016, 2016.

Kübbeler, M., Hildebrandt, M., Meyer, J., Schiller, C., Hamburger, Th., Jurkat, T., Minikin, A., Petzold, A., Rautenhaus, M., Schlager, H., Schumann, U., Voigt, C., Spichtinger, P., Gayet, J.-F., Gourbeyre, C., and Krämer, M.: Thin and subvisible cirrus and contrails in a subsaturated environment, Atmospheric Chemistry and Physics, 11, 5853-5865, doi:10.5194/acp-11-5853-2011, 2011.

Lawson, R. Paul, Andrew J. Heymsfield, Steven M. Aulenbach, et Tara L. Jensen. « Shapes, sizes and light scattering properties of ice crystals in cirrus and a persistent contrail during SUCCESS ». Geophysical research letters 25, no 9: 1331–1334, 1998.

Lawson, R.P., O'Connor, D., Zmarzly, P., Weaver, K., Baker, B., Mo, Q., and Jonsson, H.: The 2D-S (stereo) probe: Design and preliminary tests of a new airborne, high-speed, high-resolution particle imaging probe. Journal of Atmospheric and Oceanic Technology 23, 1462–1477, 2006.

Lee, D.S., Pitari, G., Grewe, V., Gierens, K., Penner, J.E., Petzold, A., Prather, M.J., Schumann, U., Bais, A., and Berntsen, T.: Transport impacts on atmosphere and climate: Aviation. Atmospheric Environment 44, 4678–4734, 2010.

Legendre, P., and Legendre, L.: Numerical Ecology, 2nd English ed., 853 pp., Elsevier Science, New York, 1998.

De León, R.R., Krämer, M., Lee, D.S., and Thelen, J.C.: Sensitivity of radiative properties of persistent contrails to the ice water path. Atmospheric Chemistry and Physics. 12, 7893–7901, 2012.

Lewellen, D.C.: Analytic solutions for evolving size distributions of spherical crystals or droplets undergoing diffusional growth in different regimes. Journal of the Atmospheric Sciences 69, 417–434, 2012.

Lewellen, D.C., and Lewellen, W.S.: The effects of aircraft wake dynamics on contrail development. Journal of the Atmospheric Sciences 58, 390–406, 2001.

Liou, K.N., Takano, Y., Yue, Q., and Yang, P.: On the radiative forcing of contrail cirrus contaminated by black carbon. Geophysical Research Letters, 40, 778–784, doi:10.1002/grl.50110, 2013.

De Maesschalck, R., Jouan-Rimbaud, D., and Massart, D.L.: The Mahalanobis Distance. Chemometrics and Intelligent Laboratory Systems 50, no. 1: 1–18. doi:10.1016/S0169-7439(99)00047-7, 2010.

Meyer, J., Rolf, C., Schiller, C., Rohs, S., Spelten, N., Afchine, A., Zöger, M., Sitnikov, N., Thornberry, T. D., Rollins, A. W., Bozóki, Z., Tátrai, D., Ebert, V., Kühnreich, B., Mackrodt, P., Möhler, O., Saathoff, H., Rosenlof, K. H., and Krämer, M.: Two decades of water vapor measurements with the FISH fluorescence hygrometer: a review, Atmospheric Chemistry and Physics, 15, 8521–8538, doi:10.5194/acp-15-8521-2015, 2015.

Mishchenko, M.I., Travis, L.D., Kahn, R.A., and West, R.A.: Modeling phase functions for dustlike tropospheric aerosols using a shape mixture of randomly oriented polydisperse spheroids. Journal of Geophysical Research 102, 16831–16, 1997.

Moore, R. H., Thornhill, K. L., Weinzierl, B., Sauer, D., D'Ascoli, E., Kim, J., Lichtenstern, M., Scheibe, M., Beaton, B., Beyersdorf, A. J., Barrick, J., Bulzan, D., Corr, C. A., Crosbie, E., Jurkat, T., Martin, R., Riddick, D., Shook, M., Slover, G., Voigt, C., White, R., Winstead, E., Yasky, R., Ziemba, L. D., Brown, A., Schlager, H., and Anderson, B. E.: Biofuel blending reduces particle emissions from aircraft engines at cruise conditions, Nature, 543, 411-415, 10.1038/nature21420, 2017.

Schäuble, D., Voigt, C., Kärcher, B., Stock, P., Schlager, H., Krämer, M., Schiller, C., Bauer, R., Spelten, N., De Reus, M.., Szakáll, M., Borrmann, S., Weers, U., and Peter T.: Airborne measurements of the nitric acid partitioning in persistent contrails, Atmospheric Chemistry and Physics, 9, 8189-8197, 2009.

Schlager, H., Konopka, P., Schulte, P., Schumann, U., Ziereis, H., Arnold, F., Klemm, M., Hagen, D.E., Whitefield, P.D., and Ovarlez, J.: In situ observations of air traffic emission signatures in the North Atlantic flight corridor. Journal of Geophysical Research 102, 10739–10, 1997.

Schröder, F., Kärcher, B., Duroure, C., Ström, J., Petzold, A., Gayet, J.-F., Strauss, B., Wendling, P., and Borrmann, S.: On the Transition of Contrails into Cirrus Clouds. Journal of the Atmospheric Sciences 57, 464–480, 2000.

Schumann, U.: On conditions for contrail formation from aircraft exhausts. Meteorologische Zeitschrift, 5, 4–23, 1996.

Schumann, U., Baumann, R., Baumgardner, D., Bedka, S. T., Duda, D. P., Freudenthaler, V., Gayet, J.-F., Heymsfield, A. J., Minnis, P., Quante, M., Raschke, E., Schlager, H., Vázquez-Navarro, M., Voigt, C. and Wang, Z.: Properties of individual contrails: a compilation of observations and some comparisons, Atmospheric Chemistry and Physics, 17(1), 403–438, doi:10.5194/acp-17-403-2017, 2017b.

Schumann, U., and Heymsfield, A.: On the lifecycle of individual contrails and contrail cirrus, Meteorological Monographs, 58, 3.1-3.24, doi: 10.1175/AMSMONOGRAPHS-D-16-0005.1, 2017.

Schumann, U., Jeßberger, P., and Voigt, C.: Contrail ice particles in aircraft wakes and their climatic importance, Geophysical Research Letters, 40, 2867-2872, doi: 10.1002/grl.50539, 2013.

Schumann, U., Kiemle, C., Schlager, H., Weigel, R., Borrmann, S., D'Amato, F., Krämer, M., Matthey, R., Protat, A., Voigt, C., and Volk, C. M.: Long-lived contrails and convective cirrus above the tropical tropopause, Atmospheric Chemistry and Physics, 17, 2311-2346, doi:10.5194/acp-17-2311-2017, 2017a.

Schumann, U., Mayer, B., Gierens, K., Unterstrasser, S., Jessberger, P., Petzold, A., Voigt, C., and Gayet, J.-F.: Effective Radius of Ice Particles in Cirrus and Contrails. Journal of the Atmospheric Sciences, 68, 300–321, 2011.

Schumann, U., Penner, J.E., Chen, Y., Zhou, C., and Graf, K.: Dehydration effects from contrails in a coupled contrail-climate model, Atmospheric Chemistry and Physics, 15, 11179-11199, doi: 10.5194/acp-15-11179-2015, 2015.

Schumann, U., Kiemle, C., Schlager, H., Weigel, R., Borrmann, S., D'Amato, F., Krämer, M., Matthey, R., Protat, A., Voigt, C., and Volk, C. M.: Long-lived contrails and convective cirrus above the tropical tropopause, Atmospheric Chemistry and Physics, 17, 2311-2346, doi:10.5194/acp-17-2311-2017, 2017a.

Schumann, U., Baumann, R., Baumgardner, D., Bedka, S. T., Duda, D. P., Freudenthaler, V., Gayet, J.-F., Heymsfield, A. J., Minnis, P., Quante, M., Raschke, E., Schlager, H., Vázquez-Navarro, M., Voigt, C. and Wang, Z.: Properties of individual contrails: a compilation of observations and some comparisons, Atmospheric Chemistry and Physics, 17(1), 403–438, doi:10.5194/acp-17-403-2017, 2017b.

Seber, G. A. F.: Multivariate analysis of variance and covariance. Multivariate observations, 433–495, 1984.

Shcherbakov, V., Jourdan, O., Voigt, C., Gayet, J.F., Chauvigne, A., Schwarzenboeck, A., Minikin, A., Klingebiel, M., Weigel, R., Borrmann, S., Jurkat, T., Kaufmann, S., Schlage, R., Gourbeyre, C., Febvre, G., Lapyonok, T., Frey, W., Molleker, S., and Weinzierl, B.: Porous Aerosol in Degassing Plumes of Mt. Etna and Mt. Stromboli. Atmospheric Chemistry Physics 16, no. 18: 11883–97. doi:10.5194/acp-16-11883-2016, 2016.

Spath, Helmuth. The Cluster Dissection and Analysis Theory FORTRAN Programs Examples. Prentice-Hall, Inc., 1985.

Sussmann, R., and Gierens, K.M.: Lidar and numerical studies on the different evolution of vortex pair and secondary wake in young contrails. Journal of Geophysical Research: Atmospheres 104, 2131–2142, 1999.

Sussmann, R., and Gierens, K.M.: Differences in early contrail evolution of two-engine versus four-engine aircraft: Lidar measurements and numerical simulations. Journal of Geophysical Research: Atmospheres 106, 4899–4911, 2001.

Vazquez-Navarro, M., Mannstein, H. and Kox, S.: Contrail life cycle and properties from 1 year of MSG/SEVIRI rapid-scan images, Atmospheric Chemistry and Physics, 15(15), 8739–8749, 2015.

Voigt, C., Jessberger, P., Jurkat, T., Kaufmann, S., Baumann, R., Schlager, H., Bobrowski, N., Giuffrida, G., and Salerno, G.: Evolution of CO2, SO2, HCl, and HNO3 in the Volcanic Plumes from Etna. Geophysical Research Letters, 41, 6, 2196-2203. doi:10.1002/2013GL058974, 2014.

Voigt C., Schlager, H., Ziereis, H., Kärcher, B., Luo, B.P., Schiller, C., Krämer, M., Popp, P.J., Irie, H., and Kondo, Y.: Nitric acid in cirrus clouds, Geophysical Research Letters, 33, L05803, doi:10.1029/2005GL025159, 2006.

Voigt, C., Schumann, U., Jurkat, T., Schäuble, D., Schlager, H., Petzold, A., Gayet, J.-F., Krämer, M., Schneider, J., Borrmann, S., Schmale, J., Jessberger, P., Hamburger, T., Lichtenstern, M., Scheibe, M., Gourbeyre, C., Meyer, J., Kübbeler, M., Frey, W., Kalesse, H., Butler, T., Lawrence, M.G., Holzäpfel. F., Arnold, F., Wendisch, M., Döpelheuer, A., Gottschaldt, K., Baumann, R., Zöger, M., Sölch, I., Rautenhaus, M., and Dörnbrack, A.: In-situ observations of young contrails - Overview and selected case studies from the CONCERT campaign, Atmospheric Chemistry and Physics, 10, 9039–9056, doi:10.5194/acp-10-9039-2010, 2010.

Voigt, C., Schumann, U., Jessberger, P., Jurkat, T., Petzold, A., Gayet, J.-F., Krämer, M., Thornberry, T., and Fahey, D.: Extinction and optical depth of contrails, Geophysical Research Letters, 38, L11806, doi:10.1029/2011GL04718, 2011.

Voigt, C., Jessberger, P., Jurkat, T., Kaufmann, S., Baumann, R., Schlager, H., Bobrowski, N., Giuffrida, G., and Salerno, G.: Evolution of CO2, SO2, HCl, and HNO3 in the Volcanic Plumes from Etna. Geophysical Research Letters, 41, 6, 2196-2203. doi:10.1002/2013GL058974, 2014.

Voigt, C., Schumann, U., Minikin, A., Abdelmonem, A., Afchine, A., Borrmann, S., Boettcher, M., Buchholz, B., Bugliaro, L., Costa, A., Curtius, J., Dollner, M., Dörnbrack, A., Dreiling, V., Ebert, V., Ehrlich, A., Fix, A., Forster, L., Frank, F., Fütterer, D., Giez, A., Graf, K., Grooß, J.-U., Groß, S., Heimerl, K., Heinold, B., Hüneke, T., Järvinen, E., Jurkat, T., Kaufmann, S., Kenntner, M., Klingebiel, M., Klimach, T., Kohl, R., Krämer, M., Krisna, T. C., Luebke, A., Mayer, B., Mertes, S., Molleker, S., Petzold, A., Pfeilsticker, K., Port, M., Rapp, M., Reutter, P., Rolf, C., Rose, D., Sauer, D., Schäfler, A., Schlage, R., Schnaiter, M., Schneider, J., Spelten, N., Spichtinger, P., Stock, P., Walser, A., Weigel, R., Weinzierl, B., Wendisch, M., Werner, F., Wernli, H., Wirth, M., Zahn, A., Ziereis, H., and Zöger, M.: ML-CIRRUS - The airborne experiment on natural cirrus and contrail cirrus with the high-altitude long-range research aircraft HALO, Bulletin of the American Meteorological Society, doi: 10.1175/BAMS-D-15-00213, 2017.

Xie, Y., Yang, P., Gao, B.-C., Kattawar, G.W., and Mishchenko, M.I.: Effect of ice crystal shape and effective size on snow bidirectional reflectance. Journal of Quantitative Spectroscopy and Radiative Transfer 100, 457–469, 2006.

Xie, Y., Yang, P., Kattawar, G.W., Minnis, P., and Hu, Y.X.: Effect of the inhomogeneity of ice crystals on retrieving ice cloud optical thickness and effective particle size. Journal of Geophysical Research: Atmospheres (1984–2012) 114, 2009.

Yang, P., Hong, G., Dessler, A.E., Ou, S.S., Liou, K.-N., and Minnis, P.: Contrails and induced cirrus: Optics and radiation. Bulletin of the American Meteorological Society 91, 473–478, 2010.

Ziereis, H., Schlager, H., Schulte, P., Velthoven, P. van, and Slemr, F.: Distributions of NO, NO x, and NO y in the upper troposphere and lower stratosphere between 28 and 61 N during POLINAT 2. Journal of Geophysical Research: Atmospheres (1984–2012) 105, 3653–3664, 2000.

Zöger, M., Afchine, A., Eicke, N., Gerhards, M-T., Klein, E., McKenna, D.S., Mörschel, U., Schmidt, U., Tan, V., Tuitjer, F., Woyke, T., Schiller, C. : Fast in situ stratospheric hygrometers: A new family of balloon-borne and airborne Lyman alpha photofragment fluorescence hygrometers. Journal of Geophysical Research: Atmospheres, 104, 1807-1816, 1999.